scientific reports

Check for updates

OPEN

Multitemporal monitoring of paramos as critical water sources in Central Colombia

Cesar Augusto Murad[1]✉, Jillian Pearse[2]✉ & Carme Huguet[3]

Paramos, unique and biodiverse ecosystems found solely in the high mountain regions of the tropics, are under threat. Despite their crucial role as primary water sources and significant carbon repositories in Colombia, they are deteriorating rapidly and garner less attention than other vulnerable ecosystems like the Amazon rainforest. Their fertile soil and unique climate make them prime locations for agriculture and cattle grazing, often coinciding with economically critical deposits such as coal which has led to a steady decline in paramo area. Anthropic impact was evaluated using multispectral images from Landsat and Sentinel over 37 years, on the Guerrero and Rabanal paramos in central Colombia which have experienced rapid expansion of mining and agriculture. Our analysis revealed that since 1984, the Rabanal and Guerrero paramos have lost 47.96% and 59.96% of their native vegetation respectively, replaced primarily by crops, pastures, and planted forests. We detected alterations in the spectral signatures of native vegetation near coal coking ovens, indicating a deterioration of paramo health and potential impact on ecosystem services. Consequently, human activity is reducing the extent of paramos and their efficiency as water sources and carbon sinks, potentially leading to severe regional and even global consequences.

Keywords Paramo, Land cover change, Landsat, Sentinel-2, Ecosystem services, Coking

High-elevation mountain ecosystems, referred to as 'paramos' in the Andes, thrive in the mountain ranges of Central and South America[1–3]. Colombia boasts the lion's share, with thirty-seven paramos encompassing approximately 2% of the country's territory[4]. Paramos provide 70% of Colombia's potable water supply and are crucial for regulating the water cycle and regional climate, as well as for capturing and storing atmospheric carbon on long timescales[3,5,6]. Their resilience in arid conditions is attributed to their efficient harnessing of water from the atmosphere, facilitated by intricate structures in plants like the Espeletia genus, commonly known as *frailejones*. Moreover, the highly porous soil with remarkably high levels of organic matter ensures rapid water filtration, purifying it before it forms the headwaters of many Colombian rivers. These remarkable attributes underscore the vital role of paramos in sustaining ecosystems and human life.

Despite their significance, the lack of a precise and universally accepted definition for paramos makes them challenging to protect. Various criteria have been used to define their boundaries[1], ranging from functional[7–9], biogeographical[10], and anthropogenic perspectives, such as traditional land uses[11]. Consequently, pinning down the exact definition of paramo has proven elusive[12]. For example, while *frailejones* are often associated with the paramo ecosystem in South America, not all paramos host *frailejones*, and areas with *frailejones* may not necessarily qualify as paramos[13]. Attempts to establish an altitude-based lower limit of 2800 mamsl as a defining parameter have been made[14], but the altitude of paramo vegetation varies across different mountain ranges and climatic zones in Colombia[4,15], making a generalized altitude-based definition impractical[16]. This ambiguity surrounding the paramo's definition opens the door to biased interpretations, favouring mining and agricultural activities within these ecologically fragile ecosystems.

The same attributes that make paramos essential water suppliers also make them attractive for coal mining, agriculture, and cattle grazing, leading to extensive occupation and settlement over the past several decades[6,17–19]. These activities raise alarms as they require the clearance of water-harnessing native paramo vegetation, which under anthropic pressure can become carbon sources instead of sinks[5]. Additionally, paramos are highly susceptible to the impacts of climate change, with studies indicating accelerated warming rates compared to

[1]Geosciences Department, Universidad de Los Andes, 111711 Bogotá, Colombia. [2]Earth Science Department, California State University, Long Beach, CA 90840, USA. [3]Environmental Sciences and Sustainability Department, Science & Technology School, IE University, 40003 Segovia, Spain. ✉email: ca.murad968@uniandes.edu.co; Jillian.Pearse@csulb.edu

lower-elevation areas[3,20]. This confluence of effects portends a grim future for paramos unless robust preservation measures are undertaken.

Understanding the nature and rates of change in paramos is crucial for devising effective protection strategies, and remote sensing provides a cost- and time-effective means to monitor rapid land use and land cover (LULC) transformations[21,22], and investigate the socioeconomic drivers behind them[23,24]. Given the escalating human pressures, land use changes, disturbances, and climate change, the wide coverage and non-invasive nature of satellite-based change detection makes it an ideal monitoring tool in threatened environments[22]. Additionally, remote sensing's ability to provide comprehensive, continuous, and frequent observations generates extensive datasets which are invaluable for supporting research on ecosystem properties, functions, and processes, thereby contributing to our understanding and preservation of paramo ecosystems[25]. It is surprising, then, that these tools have only been applied recently to paramo ecosystems in Colombia[26–28], and that a comprehensive case-specific assessment has yet to be carried out and a land cover class identified specifically for paramo vegetation.

This study aims to quantify changes in LULC in Colombia's paramos, focusing on the densely inhabited central region, home to the Guerrero and Rabanal paramos. This area has experienced rapid expansions in both agriculture and coal mining activities since the 1940s[29]. Utilizing Landsat and Sentinel-2 images from 1984 to 2021, a comprehensive change detection analysis is conducted, focusing on quantifying native paramo vegetation loss, including *frailejones*. Adopting the Environment Ministry's altitude-based definition from 2016 as a framework for delineating the paramos' boundaries, we analyze changes in paramo vegetation extent within those boundaries and examine non-LULC alterations, such as the effects of open coal-coking ovens in the proximity of paramo Rabanal. Given the robust correlation between coal mining activities and paramo locations, our findings have potential implications for all paramos neighboring these activities, shedding light on the broader vulnerability of paramo well-being. Additionally, given the ubiquity of climate change, our outcomes are relevant for paramo-like ecosystems worldwide, despite variations in local economic activities. The methodology employed in this study can be applied to any ecosystem, providing a benchmark for future research endeavors and a platform to steer conservation policy.

Materials and methods

Study area

The present study focuses on the Rabanal and Guerrero paramos of the Cundiboyacense Plateau (*Altiplano*) in the Eastern Cordillera of Colombia (Fig. 1). The plateau altitude ranges from 2500 and 2800 mamsl, and is surrounded by mountains of up to 4000 m, where paramo ecosystems are found[30]. The departments of Boyacá and Cundinamarca have the largest share of paramo area in the country, with 4172 km^2 of protected area under the paramo category[31], of which paramo Rabanal and Guerrero comprise 110.96 (2.6%) and 364.02 (8.7%) km^2, respectively.

Temperatures in this area are mainly controlled by altitude, with an annual average of ~ 14 °C, and annual variation of less than 1 °C[32]. At higher elevations average temperatures decrease, ranging from 8 to 10 °C[33] and 4 to 10 °C[34] in the Rabanal and Guerrero paramos, respectively. While annual variability is low, there are large daily fluctuations: temperatures in a single day can oscillate from 0 to 24 °C[35,36]. The annual rainfall in the region varies from 600 to 1500 mm, with a strong spatial variation and bimodal oscillation (April–June and October–December) mostly determined by the intertropical convergence zone migration (ITCZ)[30,37].

The cold and humid climate favors organic matter accumulation in the soil above the average 5%, resulting in denser-than-expected vegetation for the altitude[36,38,39]. Paramo vegetation has developed physiological characteristics adapted to endure the region's climate, and which are crucial for water capture and retention[40,41]. Guerrero and Rabanal are dominated by mid-paramo vegetation consisting of a matrix of *frailejones* (species from the genus *Espeletia* and *Espeletiopsis* endemic of these ecosystems), and grasses, in which scrubs, tussock grasses and herbs coalesce[42]. Also present are meadows commonly found around ponds or wetlands, lithophytes on rocky substrates and areas of high slope, coniferous plantations and high Andean forests; the latter are characterized by *Polylepis* forests, shrubs and weeds as scattered conglomerates, forming a transition zone between the forest and the paramo itself[43].

In both paramos, soils are derived from a parent material primarily composed of Upper Cretaceous and Lower Tertiary sedimentary rocks, and Quaternary sediments[44,45]. These were deposited during the regression of the Cretaceous seas and several smaller transgressive–regressive cycles that led to different associated coastal, alluvial and swamp facies and, therefore, the formation of coal beds[46–48]. Consequently, extraction of coal is common in the region, and used for export, internal consumption in heat and power applications and to produce a fuel known as coke[49,50].

Over the past few decades, dual-purpose cattle for meat and milk production as well as potato growing have been the prevailing complementary agricultural activities inside the paramo areas, which combined with the increasing food demand from urban centers, have resulted in more paramo territory being put under intensive husbandry pressure[51].

Data acquisition and image pre-processing

The acquired Landsat dataset comprised the period from 1984 to 2021 and three tiles with path and row numbers 08/56, 07/56 and 07/57, respectively. The optical datasets used in this study included Landsat 4–5 Thematic Mapper (TM), Landsat 7 Enhanced Thematic Mapper Plus (ETM+), Landsat 8 Operational Land Imager and Thermal Infrared Sensor (OLI-TIRS) and Sentinel-2 imagery (Table 1). The multitemporal Landsat dataset was downloaded from the United States Geological Survey Earth Explorer website (http://earthexplorer.usgs.gov) and corresponds to Landsat Level-2 Surface Reflectance Science Products (L2SP), an atmospherically corrected

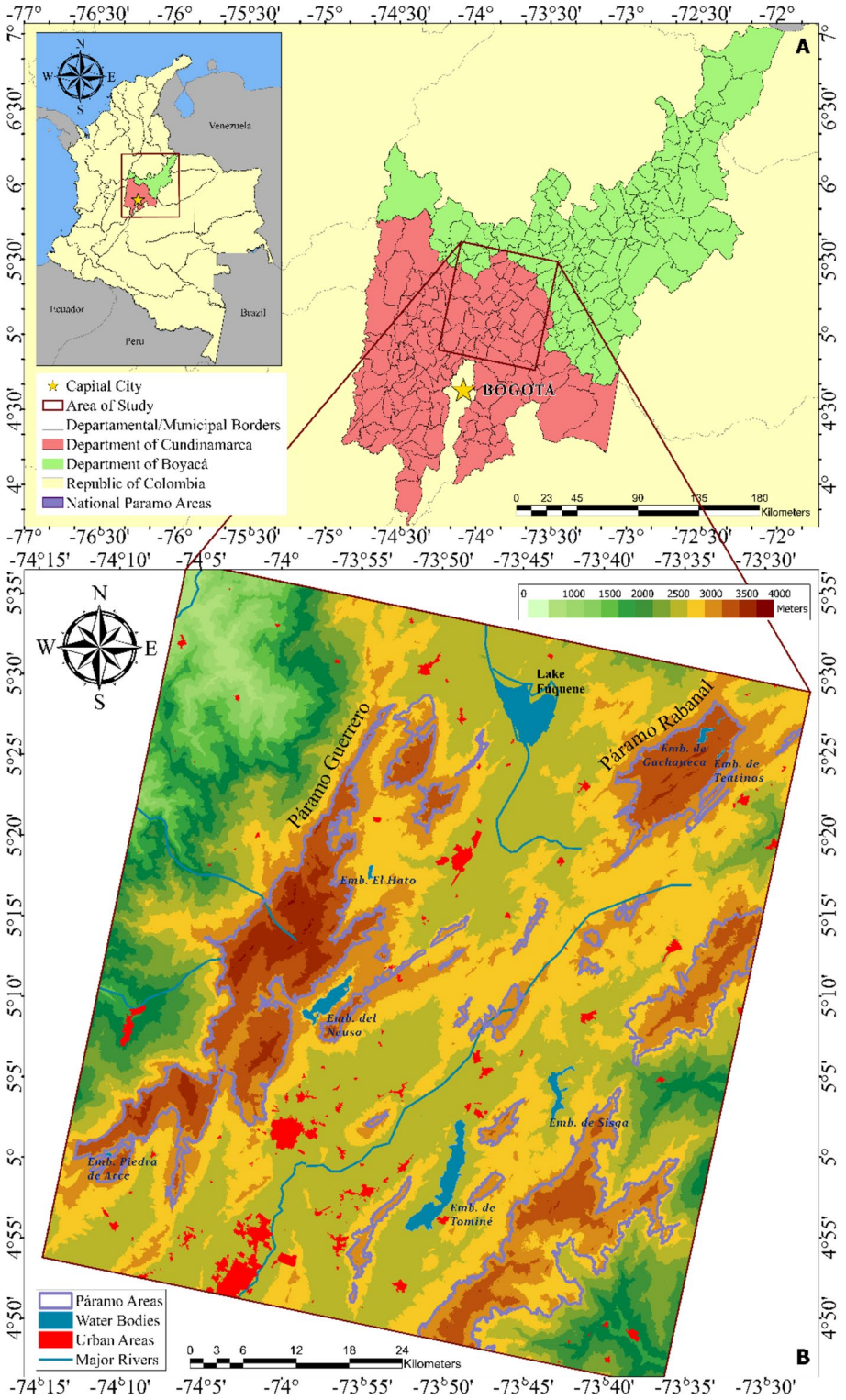

Figure 1. Map showing (**A**) the location of the departments of Boyacá and Cundinamarca and the study site within the departments and (**B**) the study site with the delineation of paramos Guerrero and Rabanal, and a Shuttle Topography Radar Mission (SRTM) digital elevation model as background. This map was produced using ArcGIS Pro Version 3.3 (https://www.esri.com/en-us/arcgis/products/arcgis-pro/overview).

imagery source for land change detection and environmental monitoring[52], generated by the Land Surface Reflectance Code (LaSRC)[53] and the Landsat Ecosystem Disturbance Adaptive Processing System (LEDAPS)[54].

Spectral bands	Landsat 4–5 TM		Landsat 7 ETM +		Landsat 8 OLI-TIRS		Sentinel 2	
	λ (μm)	Res (m)	λ (μm)	Res (m)	λ (μm)	Res (m)	λ (μm)	Res (m)
C/A	–	–	–	–	0.43–0.45	30	0.42–0.45	60
Blue	0.45–0.52	30	0.45–0.52	30	0.45–0.51	30	0.44–0.53	10
Green	0.52–0.60	30	0.52–0.60	30	0.53–0.59	30	0.53–0.58	10
Red	0.63–0.69	30	0.63–0.69	30	0.64–0.67	30	0.64–0.68	10
VRE 1	–	–	–	–	–	–	0.69–0.71	20
VRE 2	–	–	–	–	–	–	0.73–0.75	20
VRE 3	–	–	–	–	–	–	0.76–0.79	20
NIR	0.76–0.90	30	0.77–0.90	30	0.85–0.88	30	0.76–0.90	10
NIR narrow	–	–	–	–	–	–	0.84–0.88	20
Water vapor	–	–	–	–	–	–	0.93–0.95	60
Cirrus	–	–	–	–	1.36–1.38	30	1.33–1.41	60
SWIR 1	1.55–1.75	30	1.55–1.75	30	1.57–1.65	30	1.54–1.68	20
SWIR 2	2.08–2.35	30	2.09–2.35	30	2.11–2.29	30	2.07–2.31	20
TIRS 1	10.40–12.50	120 (30)	10.40–12.50	60 (30)	10.6–11.19	100	–	–
TIRS 2					11.50–12.51	100	–	–
Panchromatic	–	–	0.52–0.90	15	0.50–0.68	15	–	–
Number of bands	7		8		11		13	

Table 1. Satellite band specifications of the study. The spectral bands of each optical sensor are indicated below, with wavelength in micrometers as λ (μm) and the spatial resolution in meters (Res). *VRE* Vegetation red edge, *NIR* Near infrared, *SWIR* Shortwave infrared, *C/A* coastal aerosol, *TIRS* thermal infrared.

The Copernicus Sentinel-2 dataset was downloaded from the European Space Agency (ESA) Sentinels Scientific Data Hub (SSDH) website (https://scihub.copernicus.eu). The Sentinel-2 dataset covered the period from 2016 to 2021 and three Sentinel-2 tiles (T18NXM, T18NXL and T18NWL), corresponding to Level-1C data and Level-2A data that provides surface reflectance in all bands except the Cirrus band[55]. Since Sentinel-2 Level-2A products only became available from mid-March 2018, earlier Sentinel-2 imagery was not atmospherically corrected[56,57]. Therefore, the Sentinel-2 Level-1C images used in this research were converted from Top-Of-Atmosphere (TOA) products to Level-2A Bottom-Of-Atmosphere (BOA) reflectance products using the atmospheric correction processor Sen2Cor[57], version 2.9 with its Python language implementation.

Images were selected based on minimizing cloud cover; thus, both datasets were acquired within the low precipitation seasons (i.e., January–March and July–September). However, the constant presence of clouds in paramo altitudes makes data selection challenging, especially for a large area of interest[58]. As expected, no single cloud-free scenes were available for the study area with either sensor, so all available scenes from low-precipitation seasons with less than 30% cloud cover were employed for the present study (Supplementary Table 1A).

Corrections were applied to address cloud cover issues and image availability. These included a topographic correction to compensate for topographic bias in reflectance and a cubic convolution resampling technique to address the difference in spatial resolution between Landsat and Sentinel-2[59]. Image pre-processing and the subsequent processing was performed using ArcGIS Pro 2.8. In addition, a pixel-based image compositing approach through Google Earth Engine (GEE) was implemented to address the limitations related to image availability[60]. However, even after applying these techniques, no suitable composites were found for a small number of years (Supplementary Table 2A, Section 1A).

Image classification and change detection

A supervised image classification was performed for each image composite following a classification scheme based on the land use and land cover (LULC) classification system developed by[61]. It was defined according to the spectral variations within the same LULC class based on the land features present in the study region[26,62], and similar regions of the Ecuadorian Andes[63,64]. Moreover, since the altitudinal limits of the paramo ecosystem vary, we defined the paramo land cover based specifically on characteristic paramo vegetation[16,65,66].

Seven Level I classes were defined for the image analysis (Table 2). Based on this classification scheme, a false color IR composite was chosen as it is the standard technique for visual interpretation in vegetation mapping, and provides a clear differentiation between the LULC classes[67]. Then, a LULC supervised classification was performed using a Support Vector Machine (SVM) classification algorithm, a machine-learning methodology used for supervised classification of high-dimensional data. SVM has been shown to be reliable for the processing of remotely sensed data and superior to most of the alternative algorithms[68], as well as highly accurate for land cover change mapping[69]. The supervised classification was performed independently for each satellite to ensure consistent spectral and spatial resolution, maintaining the reliability and accuracy of the classification results by avoiding inconsistencies arising from different sensor characteristics (Table 1).

For the Landsat composites, a pixel-based classification was performed for each subset image according to the sampling scheme proposed for land classification[70], in order to define the spectral signatures representative

LULC class	Description
Montane vegetation	Dense vegetation including native forest, coniferous plantations, shrubs, and ferns
Paramo vegetation	Sparse vegetation including grasses, scrubs and *frailejones*
Agriculture	Crop fields and pastures used for farming and ranching
Water	Natural and artificial water bodies
Soil	Land areas of exposed soil
Barren	Quarries and bare ground influenced by human activity
Built-up	Densely populated and mixed urban areas, greenhouse complexes

Table 2. Land use and land cover classification scheme used in the present study based on Anderson, (1976).

of each class (Supplementary Fig. 1A). By analyzing these spectral signatures and their variability, supervised classification algorithms can accurately distinguish between different land cover types[71]. Training samples were collected by selecting homogeneous sample pixels to represent each LULC class (Table 2). In contrast, for the Sentinel-2 composites, we performed an object-based image analysis (OBIA), designed mainly for analyzing very-high-resolution (VHR) imagery, in which the image was segmented into objects for classification and analysis[72] based on spectral, spatial, textural and topological characteristics[73]. This differs from the traditional pixel-based classification, which focuses on a single pixel[74]. In this case, parameter selection for the segmentation was key to obtaining an accurate classification[70]; thus, the selection of the appropriate combination of segmentation parameters (i.e. shape, scale, smoothness and compactness) assigned to the objects was based on those suggested by[75], for Sentinel-2 images, but required further testing to ensure high accuracy of the supervised classification of individual composites.

Mixed pixels causing similarities in the spectral responses of some classes are a common problem when using data with medium spatial resolution such as that of Landsat, especially in urban areas which have a heterogeneous mix of features such as buildings, grass, roads, soil, vegetation and water, and result in noisy LULC maps[76]. To improve classification accuracy, these drawbacks were addressed using visual interpretation supported by Google Earth images and with the ERDAS Knowledge Engineer tool from ERDAS Imagine 15, to apply an expert classification system model based on hierarchical user-defined decision rules[77,78]. By incorporating additional data, the overall accuracy of LULC classification was improved[79,80]; thus, using individual band values, spatial texture analysis and spectral indices [Normalized Difference Vegetation Index (NDVI), Moisture Stress Index (MSI), Mid Infrared Index (MidIR) Modified Soil Adjusted Vegetation Index (MSAVI)], the misclassified pixels resulting from the initial classification were re-evaluated and properly reclassified, then confirmed using visual interpretation and additional false color composites. Finally, a neighborhood 3×3 majority filter was applied to each classification to recode isolated pixels responsible for noticeable salt-and-pepper effects[81].

Although field visits were conducted for visual inspection of vegetation within the study area, these did not include a comprehensive ground-truth data collection survey due to the challenging nature of surveying in this region. Instead, the accuracy assessment was conducted using randomly selected points (see Supplementary Section 2A.) supported by the original corresponding Landsat or Sentinel-2 images and, for the most recent classifications, Google Earth Images sourced between January 26 of 2016 and February 16 of 2021 at the time of the satellite image processing for the present study. Google Earth has been previously utilized as an alternative source for ground truth data when field data was not available, thereby aiding in the validation and accuracy assessment of land cover classifications derived from remote sensing data[82]. We recognize that discrepancies in the dates of Google Earth imagery could introduce changes in land cover and environmental conditions, potentially impacting the validation process's accuracy and precision. Nevertheless, Google Earth data has been demonstrated to be a reliable and cost-effective reference for land cover maps, making it a viable alternative to more expensive or time-consuming high-resolution data[83].

This process was further supported by extensive knowledge of the study area acquired through prior field visits to the Fúquene lagoon and coking oven locations, and observation of the distinguished classes, including agricultural activities, montane vegetation and native paramo vegetation along with forest plantations and invasive species (*Gorse*). Large parts of the study area were difficult to access due to private property restrictions, so observations were instead made near accessible roadsides. Moreover, given the lack of availability of historical ground-truth data or high-resolution aerial photography, we assumed the long-term temporal stability of spectral responses to allow for historical classifications to inform land cover mapping efforts[71]. This approach mitigates potential biases, ensuring that the accuracy of past classifications is reasonably inferred based on recent data and field observations[79]. Further validation of our results was conducted through a review of available land cover and land use datasets, focusing on the 30-m annual maps (1985–2022) of the Colombia MapBiomas project (https://colombia.mapbiomas.org/) for Landsat classifications, and the 10-m annual land cover/land use maps (2017–2023) of the ESRI Living Atlas (https://livingatlas.arcgis.com/landcover/) for Sentinel-2 classifications.

Multi-temporal satellite imagery is used to detect and monitor changes in ecosystems by comparing a pair of classified images from two different time periods[84], ultimately in the form of land cover change maps. Nonetheless, change maps are subject to the same errors as the input classifications[85], so we used a Post-Classification Comparison (PCC) change extraction algorithm to compare the classified images and produce a change matrix showing quantitative "from-to" changes. This cross-tabulation analysis simplifies the calculation of the quantity of conversions from one LULC class to another over the period evaluated[86] and can be visually displayed as a change detection map to facilitate interpretation[87]. As a result, change detection maps were produced for each

paramo, showing a total of 30 "from-to" change categories. For a better map visualization, the number of categories was reduced by merging LULC that changed into a same class, while LULC classes that did not change were not displayed. Afterwards, an accuracy assessment of each classification and change detection map was performed along with their respective confidence intervals (see Supplementary Section 2A). The methodology adopted in this study is summarized in Fig. 2.

To account for the effects of human intervention that do not result in vegetation cover changes, we also monitored vegetation health and vigor changes. We employed band combinations using Landsat and Sentinel-2 SWIR-1, SWIR-2, NIR and red bands, specifically the False Color and Shortwave Infrared band combinations, to identify the proximity of coking ovens to paramo Rabanal. The oven locations were identified by seeking very high temperature anomalies with respect to the background, often visible in vivid red color[88], which has proved to be useful in detecting hotspots and fire spots with both Landsat[89] and Sentinel-2 imagery[90]. Together with variations in the spectral response of the paramo vegetation in the multispectral images, potential alterations in the health of the vegetation within the paramo area was assessed.

Results

Classification and change detection

We observed a remarkable increase in montane vegetation, while paramo vegetation decreased. Agriculture, urban developments, soil, and barren terrains showed subtler shifts (Figs. 3 and 4). Suesca and Fúquene lagoons experienced a noticeable reduction in their surface area (Fig. 1), whereas the reservoirs of Tominé, Neusa and Sisga, as well as other non-lagoon water bodies within the paramos, were surprisingly resistant to change. The

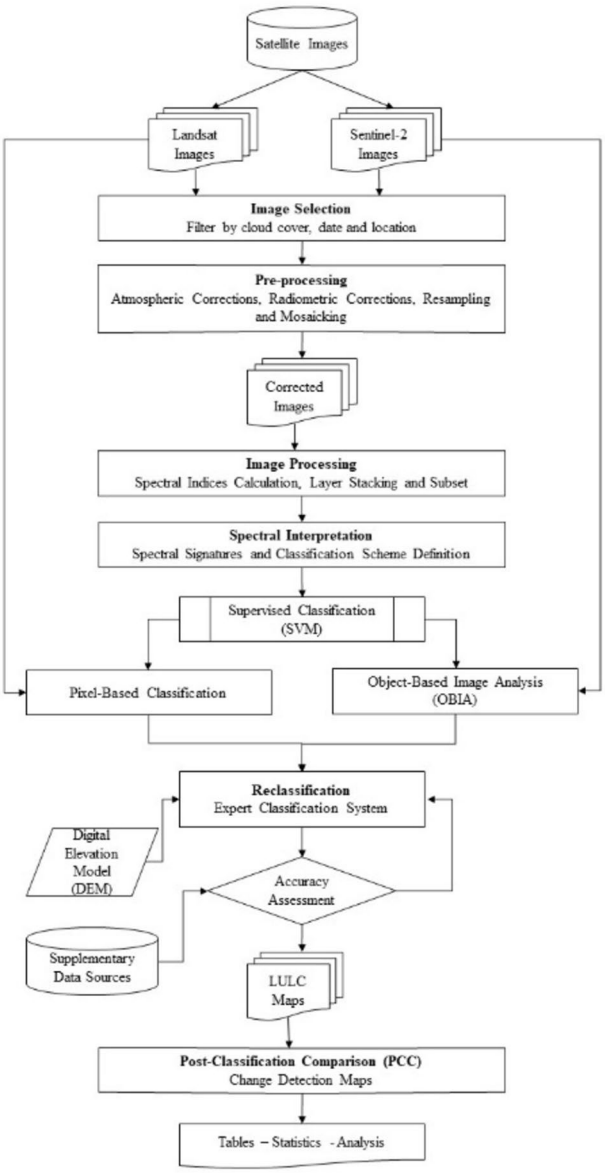

Figure 2. Methodological flowchart of the data processing.

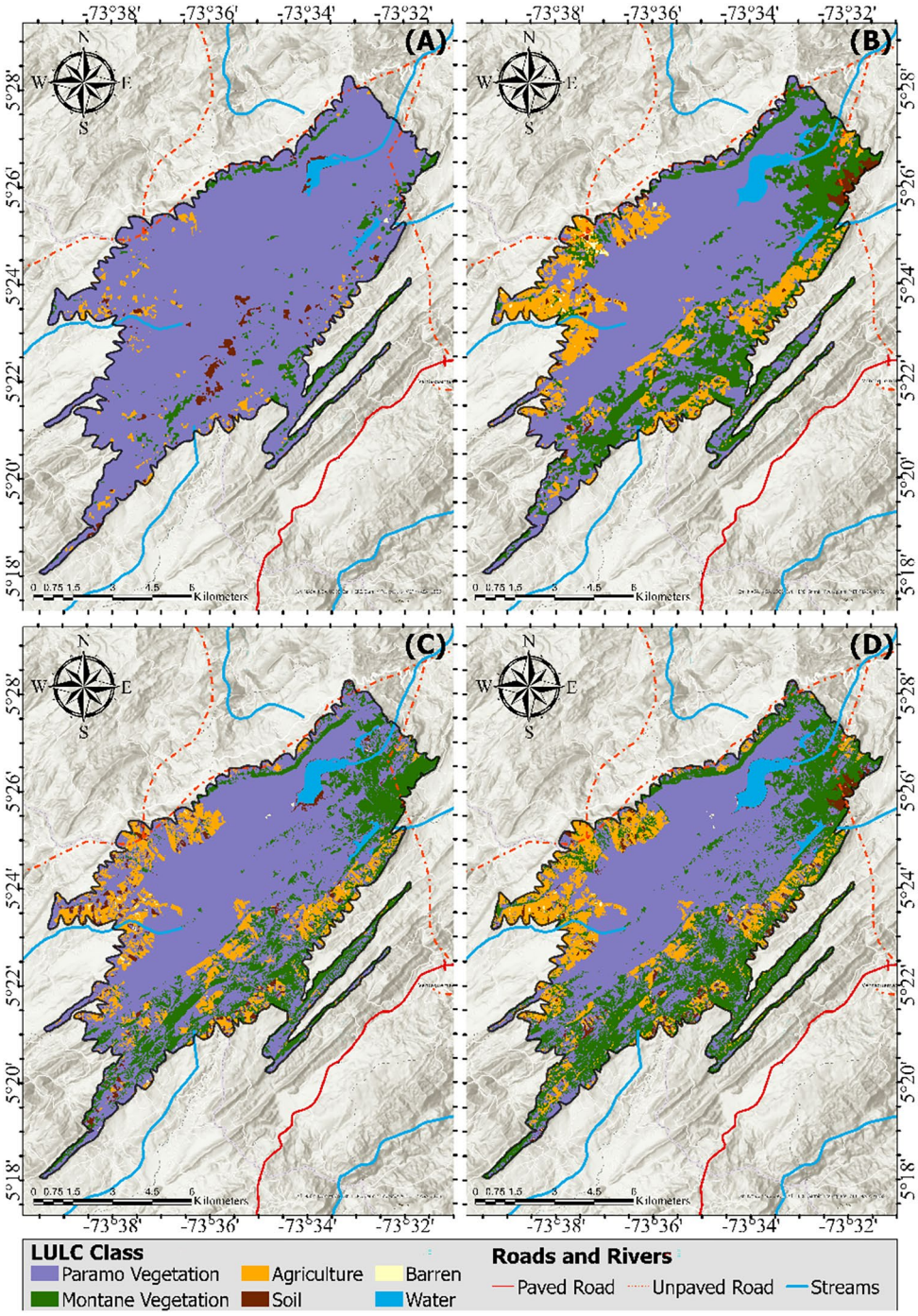

Figure 3. Land use and land cover (LULC) thematic maps of the delimited area of paramo Rabanal corresponding to the Landsat and Sentinel supervised classifications at the initial and final years of the period of study. Each of the four panels display the main LULC classes along with the local water bodies (blue) and road network (red), and a topography basemap. (**A**) Landsat-4/5 1984 (**B**) Landsat-8 2021 (**C**) Sentinel-2 2016 (**D**) Sentinel-2 2021. This map was produced using ArcGIS Pro Version 3.3 (https://www.esri.com/en-us/arcgis/products/arcgis-pro/overview).

temporal trends of the LULC classes were analyzed by evaluating different models to characterize these trends comprehensively, focusing on those which experienced significant land cover changes[91–93]. Strong positive and negative trends for vegetation-related classes were evident regardless of trend model, and further supported by the Cox-Stuart statistical test for trend detection[94] (Supplementary Tables 14A and 15A, Section 4A).

Water bodies, soil and barren land did not show any major changes in cover area over time, and no urban development was detected inside the paramos since the beginning of the study period. However, when assessing

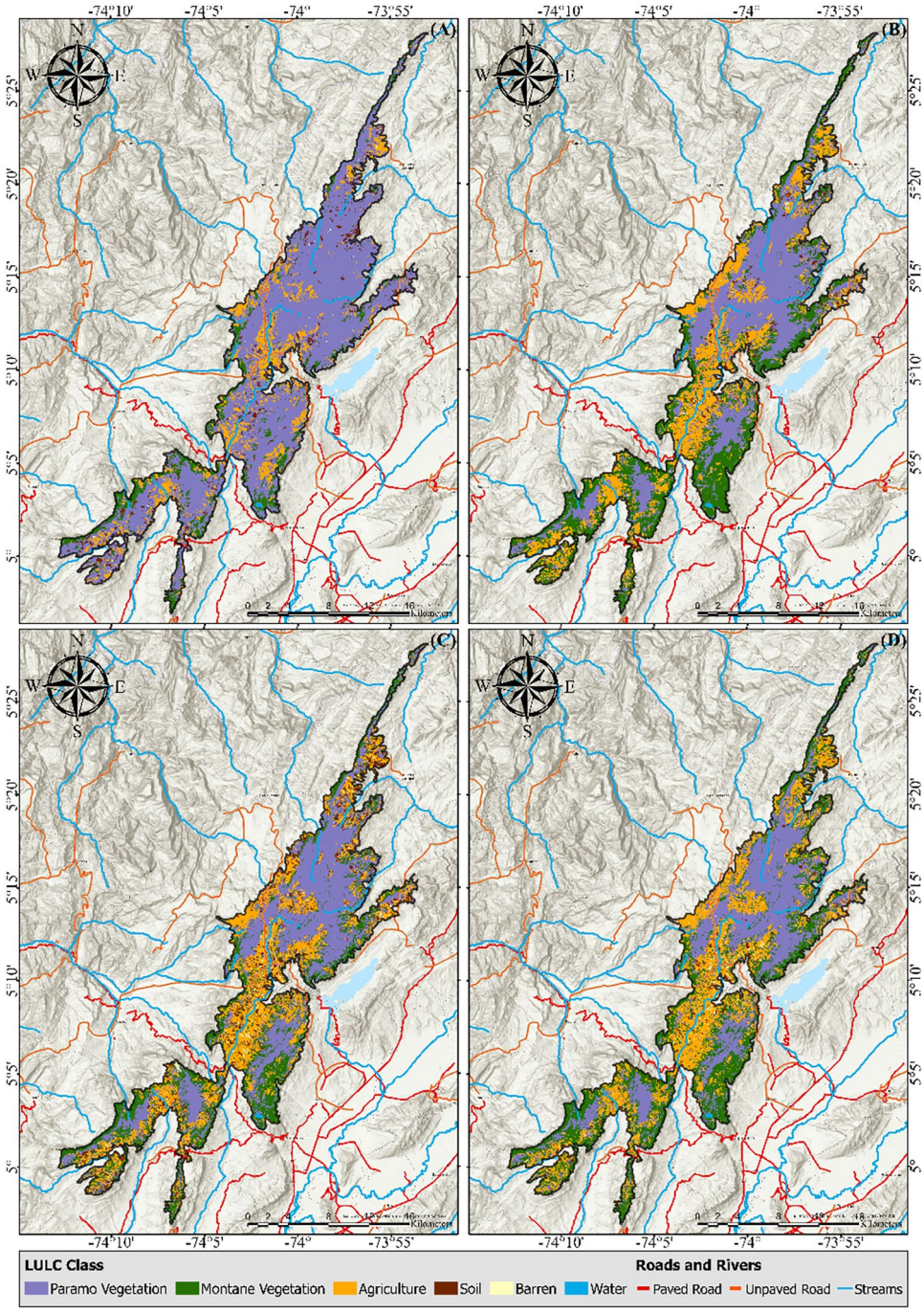

Figure 4. Land use and land cover (LULC) thematic maps of the delimited area of paramo Guerrero corresponding to the Landsat and Sentinel supervised classifications at the initial and final years of the period of study. Each of the four panels display the main LULC classes along with the local water bodies(blue) and road network (red), and a topography basemap. (**A**) Landsat 1984 (**B**) Landsat 2021 (**C**) Sentinel-2 2016 (**D**) Sentinel-2 2021. This map was produced using ArcGIS Pro Version 3.3 (https://www.esri.com/en-us/arcgis/products/arcgis-pro/overview).

each paramo separately, we found strong trends in the changes between LULC classes, portrayed in the corresponding thematic maps of the classification (Figs. 3 and 4). In the case of Rabanal (Fig. 3), montane vegetation exhibited a persistent increase along an approximately logarithmic trend, rising by 19.5% from 1984 to 2021, which translates to an average 4.5% annual rate of change and a land cover expansion of 21.7 km^2. Agriculture inside the paramo increased by 12.5% during this period, with an average annual rate of change of 4.9%, with a quadratic trend that suggests an increasing rate of agricultural expansion. In contrast, paramo vegetation

showed an astonishing 33.8% decrease since 1984, corresponding to an average annual rate of change of 1.3% and a strong negative trend.

Parallel trends were observed for the major LULC classes in paramo Guerrero (Fig. 4), though on a larger scale since Guerrero is about 3 times larger than Rabanal. An increase of montane vegetation area by 20.2%, transforming a landscape area that spanned 73.7 km^2 (an average annual rate of change of 3.2%), with the largest increase observed between 1988 and 1990. At the same time a staggering 110.4 km^2 or 30.3% of paramo vegetation was lost, with the most significant reduction occurring between 1989 and 1991, equivalent to an average annual rate of change of − 1.5%. Agriculture showed a moderate positive trend growing by 41.2 km^2 (1.6% annual change rate), with most expansion occurring between 1988 and 2000. The average annual rates of change varied between periods, with the timespan between 1984 and 1991 showing considerably greater changes compared to later years.

Sentinel-2 classifications confirmed these tendencies: between 2016 to 2021, while agricultural land use showed a slight change, montane vegetation increased by 43.89% in paramo Rabanal and by 40.64% in paramo Guerrero. These changes represent striking average annual growth rates of 8.77% and 8.12%, respectively. Meanwhile, paramo vegetation showed strong negative trends with a 11.5% reduction in Rabanal (average annual decline of − 4.1%), while paramo Guerrero saw a 4.7% decrease of its native vegetation (average annual rate of change of − 2.4%). Consequently, declining paramo vegetation mirrored a surge in montane vegetation and agricultural lands (Fig. 5). The remainder of the LULC classes remained largely unaltered throughout the entire study period.

Landsat and Sentinel-2 classifications clearly distinguished paramo vegetation from agriculture and montane vegetation. Nonetheless, Landsat classifications revealed a greater extent of paramo vegetation and less montane vegetation compared to Sentinel-2 classifications, probably because of the heterogeneity of classes[95], and the detection of small-scale features in the higher resolution data[96]. Sentinel-2 classifications clearly indicated a larger paramo vegetation loss by 2021 compared to the Landsat classifications, showing an additional 5.3% and 5% paramo vegetation loss inside paramos Rabanal and Guerrero areas, respectively, which is consistent with the continuous loss trend of paramo vegetation and gain in montane vegetation observed in both paramos over the entire study period.

It should be noted that a considerable portion of the study regions—56.9% (210 km^2) in Guerrero, and 60.9% (68.7 km^2) in Rabanal—remained unaltered since 1984. Nonetheless, when considering the paramo vegetation cover alone, 47.2% in Guerrero and 39.2% in Rabanal were converted into forest and agricultural land (Fig. 6).

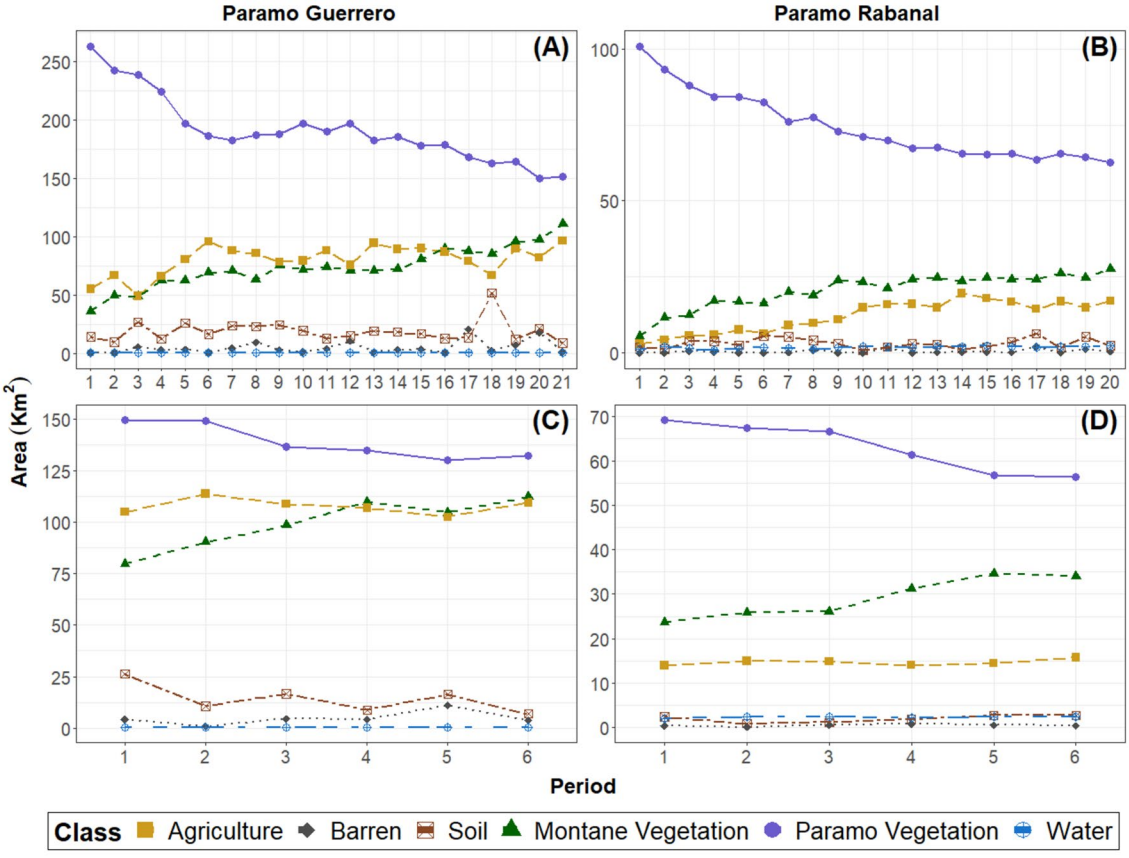

Figure 5. Land use and land cover development inside the paramos Guerrero and Rabanal for Landsat (**A**,**B**) and Sentinel-2 (**C**,**D**) supervised classifications, which determine the contrast in the sensor's temporal resolutions. Each period corresponds to the time span between two different classifications with subsequent acquisition years (refer to Supplementary Table 2A).

These shifts corresponded to 73.3% and 83.5% of the total quantified change since 1984 in Guerrero and Rabanal, respectively. There was also a transition of paramo soils to agricultural use; this shift accounted for 2.54% and 5.29% of the total quantified change in Guerrero, and 5.1% and 20.1% in Rabanal, based on the respective classifications derived from Landsat and Sentinel-2 (Fig. 5). Built-up areas did not show significant change into other LULC classes, and as for soil and barren land, the major changes observed were between each other and to-and-from agricultural use. A comprehensive compilation of change detection statistics for both paramos and both sensors is presented in the Supplementary Information, in the form of percentages and areas of each "from–to" transition (see Supplementary Tables 5A, 6A and 7A for details).

Landsat-based change detection analysis from 1984 to 2021 in paramo Guerrero showed that a total of 158.9 km^2 underwent transformation during this time frame, mostly loss of paramo vegetation, which accounted for 116 km^2 (Fig. 6). Nearly 42% (66.1 km^2) of the original paramo vegetation was replaced by montane vegetation. Another 31.7% (50.3 km^2) of the paramo vegetation was replaced by agricultural activities. Other changes included the shift from agriculture to montane vegetation (6.9%) and the transformation from soil to agriculture (5.1%) (see Supplementary Tables 5A and 6A). The remaining "from–to" change categories, each representing less than 5% of the total change, did not yield significant insights.

Rabanal experienced substantial LULC transformations between 1984 and 2021. A significant proportion of the transformed area consisted of the conversion of paramo vegetation to montane vegetation and agriculture, accounting for 51.5% (22.6 km^2) and 32% (14.1 km^2) of the total change (43.9 km^2), respectively. An additional 4.1% of the total change encompassed the conversion of paramo vegetation to soil, while the remaining "from–to" change categories individually represented less than 3% of the total change. A large portion of the land within the paramo area, comprising 68.7 km^2 or 61%, remained unchanged throughout the study period. The percent change from paramo vegetation to other LULC classes is illustrated in Fig. 7 for every period within both paramos. Each period corresponds to the time interval between two different supervised classifications, as denoted in the Supplementary Table 2A.

Change detection analysis from Sentinel-2 showed the same tendencies within the paramo areas of Rabanal and Guerrero during the 5-year interval from 2016 and 2021. Again, the most substantial transformation observed was paramo vegetation being replaced by montane vegetation, constituting 43.6% (11.1 km^2) and 29.5% (23 km^2) in Rabanal and Guerrero, respectively. However, there were nuanced variations in secondary changes: for Rabanal, the runner-up was the shift from paramo vegetation to agriculture, accounting for 16.3% of the altered landscape (Fig. 8), while in Guerrero, the transformation of soil into agricultural use represented

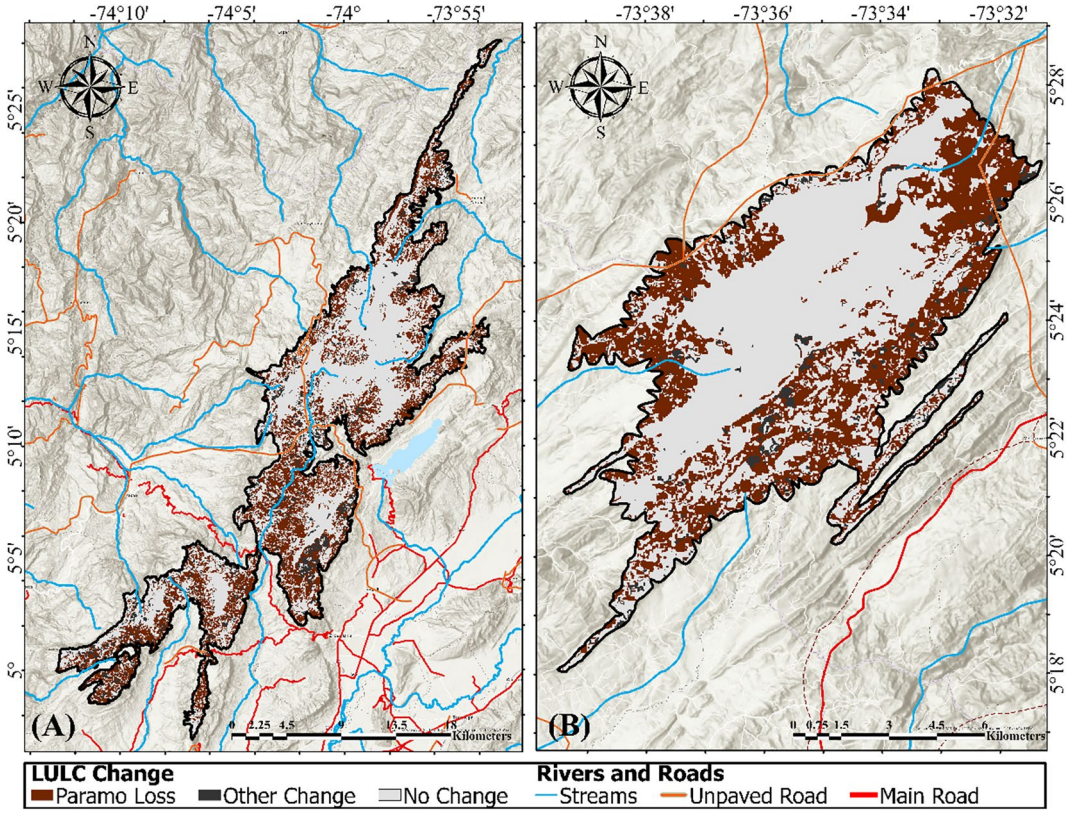

Figure 6. Change detection maps highlighting areas of paramo land cover loss between 1984 and 2021, as well as other land cover changes along with the local water bodies and road network, with a topographic basemap as background, for (**A**) Paramo Guerrero and (**B**) Paramo Rabanal. This map was produced using ArcGIS Pro Version 3.3 (https://www.esri.com/en-us/arcgis/products/arcgis-pro/overview).

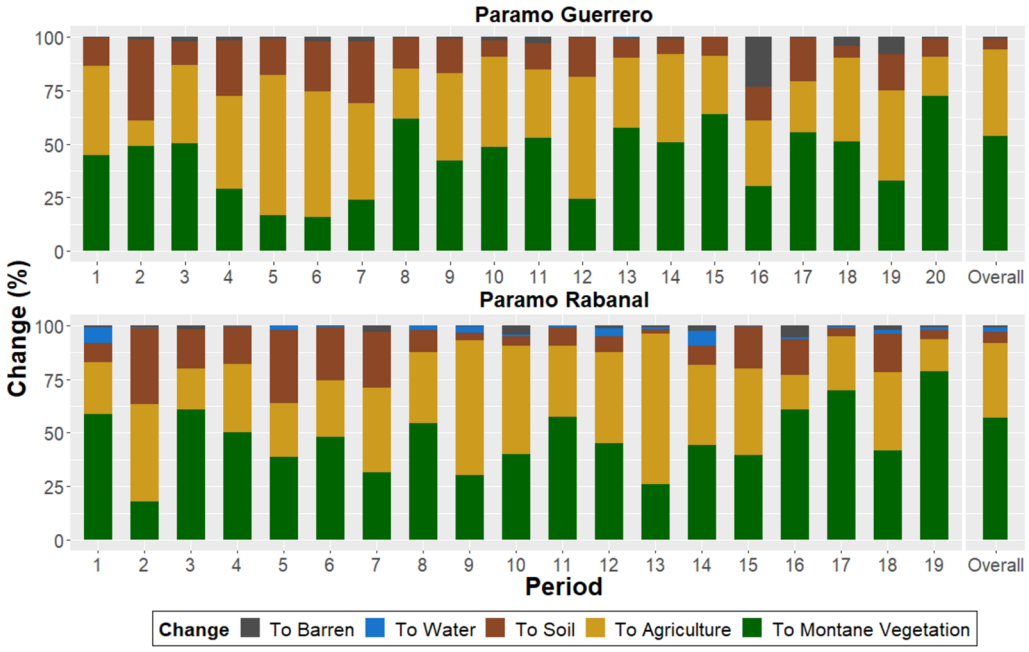

Figure 7. Bar charts depicting paramo land cover transformation to other LULC classes, in terms of percentage (%), corresponding to the Landsat change detection analysis for both paramos Rabanal and Guerrero over the study period. Each period corresponds to the time range between two different classifications with subsequent acquisition years. For the period's timespan refer to Supplementary Table 2A.

the second-most substantial alteration at 20.1%. It is worth emphasizing that despite these notable changes, the majority of the paramo areas in both Rabanal and Guerrero remained unaltered during this briefer period, with 77.2% and 78.6% of these sensitive landscapes retaining their LULC classification between 2016 and 2021. Figure 7 provides a year-by-year breakdown of percent change from paramo vegetation to other LULC classes.

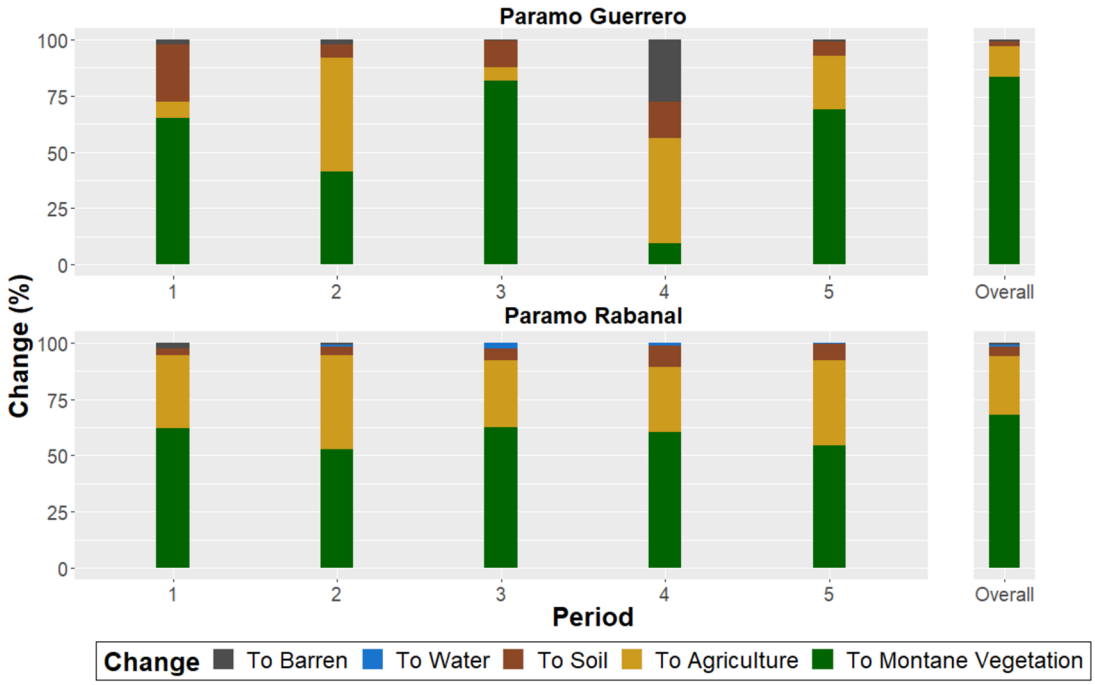

Figure 8. Bar charts depicting paramo land cover transformation to other LULC classes, in terms of percentage (%), corresponding to the Sentinel-2 change detection analysis for both paramos Rabanal and Guerrero over the study period. Each period corresponds to the time range between two different classifications with subsequent acquisition years. For the period's timespan refer to Supplementary Table 2A.

Accuracy assessment

High accuracy was obtained for all the classifications, with overall accuracies ranging from 93.8 to 97.9% and Kappa values between 0.88 and 0.97 (Supplementary Tables 3A and 4A). Supervised classifications of both Landsat and Sentinel images exhibited low omission errors with producer's accuracies over 80% in all classes, except in the Soil and Barren classes, which presented lower values (but above 60%) in various instances, particularly for Rabanal. Similarly, high user's accuracies indicated low commission errors, except for the Barren class, which was slightly below 80% for one of the Landsat classifications of Rabanal. The heterogeneity in land cover features causing similar spectral responses of soil and barren land with sparse paramo vegetation and urban areas, respectively, reduces the measured accuracy values. The complete accuracy measures for each LULC class and their associated uncertainties are presented in the Supplementary Section 2A (Supplementary Tables 8A and 9A), along with the error-adjusted total areas of each classification (Supplementary Tables 10A and 11A). The total area values obtained for each class each year using "pixel count" differ from the error-adjusted estimated area; however, they still fall within the 95% confidence interval.

Comparison of our results with those of the MapBiomas and ESRI datasets revealed the same trends, but different LULC areas inside paramos Rabanal and Guerrero. This discrepancy can be explained by the fact these datasets use different classification schemes (as neither has a specific category for paramo vegetation), and because significant cloud cover is still present in both the MapBiomas and ESRI datasets; however, equivalent classes were identified and assessed, with paramo vegetation corresponding to other non-forest formation and rangeland classes in the MapBiomas and ESRI, respectively. The MapBiomas revealed a substantial increase in forest and agriculture areas while paramo vegetation of Rabanal and Guerrero decreased by 44.26% and 40.59% from 1985 to 2021, respectively. Similarly, ESRI displayed a reduction in paramo vegetation of 19.66% and 18.74% for Rabanal and Guerrero, respectively, accompanied by an expansion of forest areas and agriculture between 2017 and 2021.This trend agreement ensures the robustness of our cloud-free temporal mapping focused on paramos, demonstrating its value in contributing new insights for the studied region.

Likewise, a high accuracy was achieved for the change detection maps, with overall accuracies ranging from 94 to 96.8% and Kappa values between 0.90 and 0.92 (Supplementary Tables 3A and 4A). Most transitions exhibited low omission errors with producer's accuracies over 75%, but soil related changes presented lower values (above 60%) in various instances for the Rabanal thematic maps. Conversely, high user's accuracies (over 80%) indicated low commission errors for all classes of both the Landsat and Sentinel-2 change thematic maps. The total area values obtained for each change category and year using "pixel count" differ from the error-adjusted estimated area; however, they still fall within the 95% confidence interval. The complete accuracy measures for each "from-to" change category with their associated uncertainties are reported in the Supplementary Information (Supplementary Table 12A).

Detection of coke ovens

Based on a false color band combination using the SWIR, NIR and VRE-2 bands of Sentinel-2, where hot surfaces saturate the mid-IR bands, coking ovens were identified close to the paramo Rabanal boundaries, especially along the northern and western limits, where they appear on the image as bright red spots (Fig. 9). The number of detected spots has increased by 492.2% since 1984, with a total change in area from 0.02 to 0.1 km^2 by 2021. No coking ovens were found in paramo Guerrero.

We also detected a decrease in the infrared reflectance of the paramo vegetation near the coking ovens (Fig. 10). The spectral profile boxplots encompassed the pixels inside two distinct sections of the paramo: the north-western section in proximity to the nearest coke oven (within 2 km), and the south-eastern section of the paramo farther away. Visual inspection in the field confirmed that vegetation near the ovens has a coating of black soot, which is likely responsible for the change in the spectral signature.

Discussion

We found significant changes in Colombia's eastern cordillera paramos, primarily due to human influence. These changes include alterations in soil cover, reduction of native vegetation, and profound impacts from agricultural practices, coal mining, and climate change, varying across land covers and correlating with geographic features such as elevation gradients. By analysing each of these factors, we aim to characterize their individual and combined effects on paramo ecosystems. Because of the crucial ecosystem services they provide, continuous monitoring is imperative to identify ongoing patterns of change and their causes. Freely available satellite images coupled with cutting-edge processing techniques have allowed us to define a spectral signature for paramo vegetation, identify patterns and drivers of rapid land cover change, and detect potential impacts of nearby coal production on vegetation health even where land cover type is conserved.

Both paramos in the region have experienced montane vegetation encroachment, yet there are differences: Rabanal has rapidly transitioned paramo vegetation into agricultural land, while Guerrero exhibits significant soil use changes. These variations can be attributed to factors such as geographic and climate differences, as well as variations in local agricultural practices and land management. Notably, Guerrero does not have coal mining operations, which significantly influence land use patterns. These differences reflect diverse ecological, geographical, and socio-economic factors, which call for tailored conservation efforts.

Magnitude of Paramo changes

Land cover changes in vegetation above the 2800 mamsl paramo boundary have been substantial (Fig. 5)[41], and our findings agree with previous studies that report native vegetation loss and fragmentation from extraction activities, agriculture-related deforestation, and road construction[51,97], leading to adverse spatial, socioeconomic, and environmental consequences[98]. Similar encroachments have been observed in protected areas such

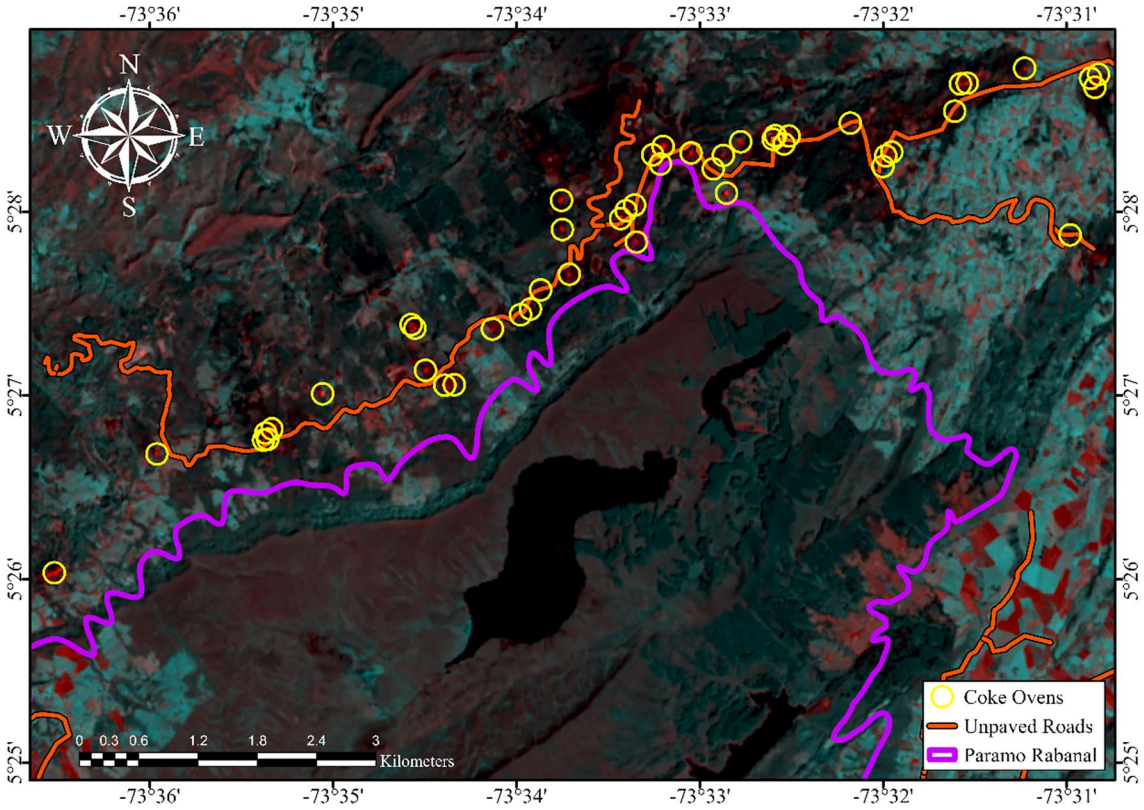

Figure 9. Map displaying a false-color image (bands 12,8,6) subset of a Sentinel-2 scene from February 13 of the year 2021 provided by the Sentinels Scientific Data Hub (SSDH) website (https://scihub.copernicus.eu), along with the local road network and the paramo boundary. Hot surfaces appear as noticeable bright red spots, which are highlighted by the yellow circles, mainly near the northern and western limits of paramo Rabanal. This map was produced using ArcGIS Pro Version 3.3 (https://www.esri.com/en-us/arcgis/products/arcgis-pro/overview).

as the Amazon[99], underscoring the broader trend of anthropogenic influence on Colombian ecosystems, while additional factors such as contamination and untreated domestic wastewater discharge further complicate the environmental landscape[100].

The apparent decrease in anthropic pressure in recent years could be explained by the recent declaration of forest reserves and modifications to paramo protection policies[101], including payment for ecosystem service programs[13,102,103]. However, the effectiveness of these measures has been questioned for some paramo areas[104], which suggests that local conditions and geological factors also influence adherence to environmental laws[105–107]. Despite regulations prohibiting mining and farming activities within paramo boundaries since 2011, weak institutional oversight coupled with past governments' push to attract foreign investment in Colombia's extractive sector, has led to a surge in mining operations, even without environmental permits, affecting 26 paramo regions and exacerbating environmental challenges[108,109]. For instance, a recent environmental impact assessment in the southwest region of Santurbán paramo showed a level of arsenic contamination which surpasses international regulatory standards[110], while coal and coking activity have been found to contaminate water, sediments, and soils near paramo Rabanal[49,100,111].

Land use changes within the paramos are not evenly distributed: over half the increase in montane vegetation and half of the newly established agricultural land was located above 2800 mamsl, where paramo vegetation is prevalent (Fig. 11). Altitude was found to be a significant determinant of ecological changes within paramo ecosystems, with lower elevations experiencing more pronounced vegetation loss. Factors such as slope inclination and climatic variations also influence alterations, highlighting the multifaceted nature of paramo dynamics and emphasizing the need for a nuanced understanding of altitude's role in driving ecological changes. This relationship between paramo change and elevation was confirmed by applying a General Additive Model. The complete statistical analysis is presented in Supplementary Section 3A (Supplementary Table 13A and Supplementary Fig. 2A).

Factors driving change

Human activity was found to be the main factor driving change: we identified agriculture and mining activities, including inefficient coking processes, as key factors in the deterioration of both paramos; which have also led to soil contamination and surface water quality decline[49]. Higher temperatures and degraded soils are likely to result in net carbon loss, alteration of catchment areas, reduced soil water and carbon retention capacity[5,112], and decreased aquifer replenishment[3,113], thereby intensifying the conflict over water resource distribution between

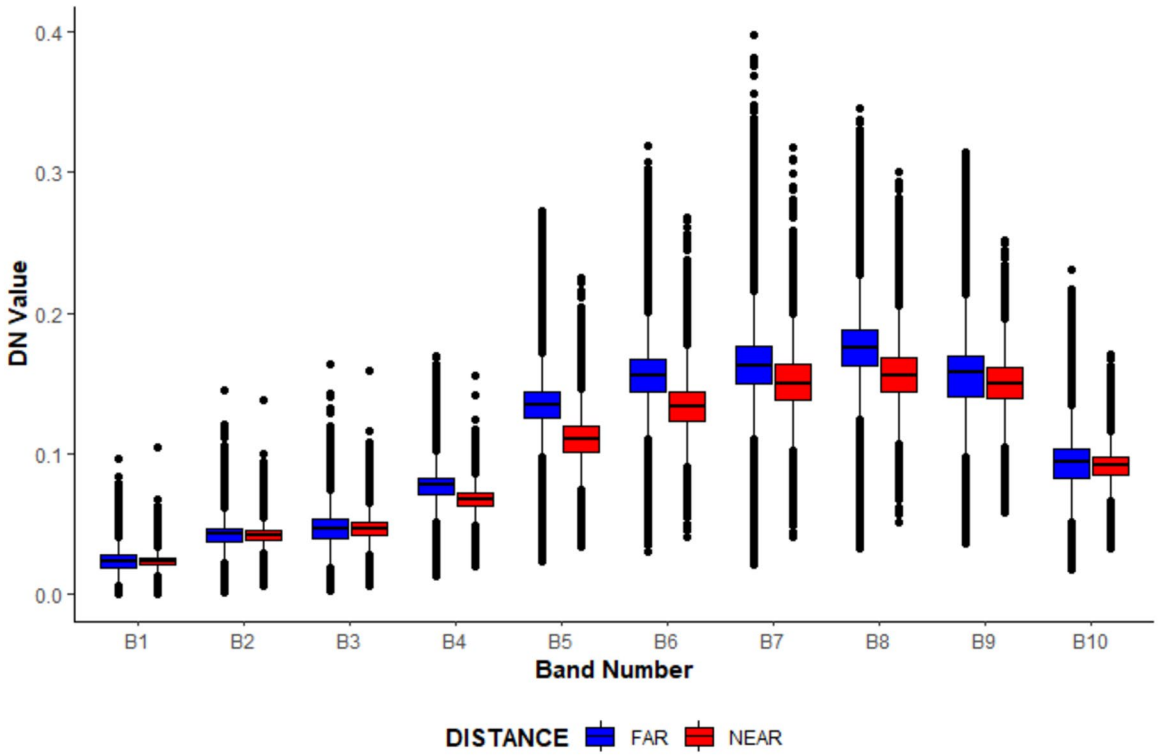

Figure 10. Spectral profile box plot of paramo vegetation inside the paramo Rabanal area for all spectral bands. Two classes based on the distance or proximity to the coking ovens are displayed. The blue boxes indicate vegetation far (south-eastern section) from the coking ovens and the red boxes indicate vegetation near (north-western section) the coking ovens.

human consumption, agriculture, and mining[3,5,114]. Water-related replacement of paramo vegetation within Rabanal can be attributed primarily to the creation of the Gachaneca reservoir[33], although seasonality effects were also detected. The Fúquene and Suesca lagoons are known to be heavily intervened, primarily by conversion of native vegetation to agricultural land, pasture, and mining systems[115]; and the accompanying increase in demand for water, mainly for irrigation, has reduced water levels in both systems[116–120]. Interestingly, many of the alterations expected from climate change mirror the impacts observed from current human activities[121].

Agriculture expansion

In both paramos, the primary human-induced alterations stemmed from the expansion of farming activities, encompassing both crop cultivation and livestock rearing. The agricultural activity includes various traditional Andean root and tuber crops. Industrial farming is not used in these areas because the terrain makes its development challenging[122]; however, many small operations have an equivalent impact when it comes to contamination and size reduction of the ecosystem[123]. This is the result of market dynamics in this region, characterized by a cyclic agriculture pattern between tuber crops and pastures[124,125], which likely explains the observed fluctuations between crop, soil, and barren land in our classifications. Since 1984, agricultural expansion in the region has primarily occurred within the paramo areas, because agriculture had already been established in the surrounding plains. This expansion, driven by population growth, involves clearing new land[126,127]; unfortunately, fallow land does not naturally revert to paramo vegetation, and *frailejones* are challenging to transplant. Therefore, intensive efforts are required to restore altered paramo, even in abandoned grazing lands[128,129].

The effects of human intervention on paramos are not limited to changes in vegetation type: the use of pesticides is an increasing source of soil and water contamination as agriculture expands and can affect the quality of the water supply in the high catchments. Furthermore, potato crop and livestock activities affect the physicochemical properties of the soils, including a reduction in carbon storage and cation exchange capacity[130].

Coal mining

Afforestation with exotic species of the genera Eucalyptus and Pinus was the predominant direct impact of nearby mining, particularly evident in Rabanal. These plantations serve as a timber source for construction material within coal mines, making them an indirect and irreversible outcome of mining activities[131], a phenomenon also reported in Ecuadorian paramos[132]. These trees demand substantially more water than native species, leading to water reserve declines[133,134], displacement of native flora and fauna, and soil sterility[135,136]. Previous studies have shown that LULC changes influence the broader climate of South America and the specific microclimate of paramo ecosystems[137,138], altering land surface albedo, thereby impacting precipitation and surface temperature.

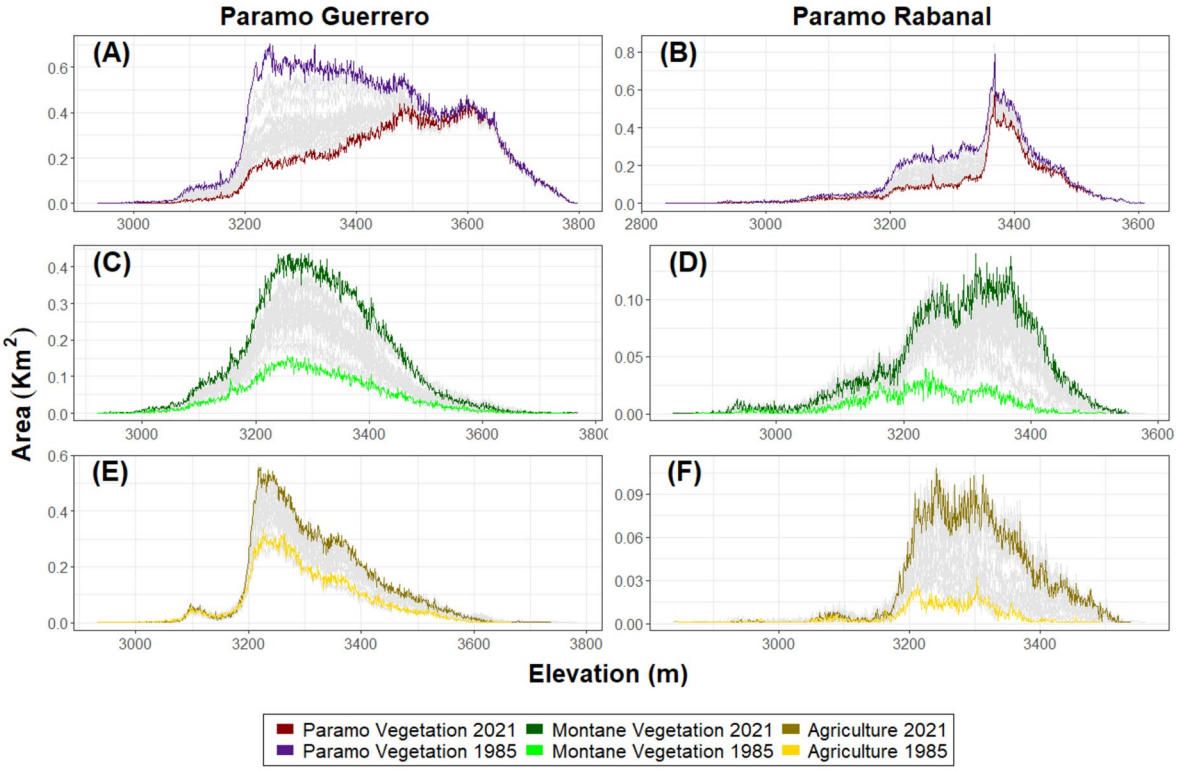

Figure 11. Land use and land cover development of paramo vegetation, montane vegetation, and agriculture in relation to the elevation. Panels (**A**) and (**B**) represent evolution of paramo vegetation, (**C**) and (**D**) depict the variation of montane vegetation, while (**E**) and (**F**) display the development of agriculture over time. Darker colors indicate the most recent supervised classification, while the lighter shades correspond to the oldest one. The color variations and patterns provide insights into the temporal changes and trends in land use and land cover within the specified vegetation types in relation to elevation.

For example, afforestation decreases reflectivity and increases radiant energy absorption[139], particularly with forest genera like Eucalyptus and Pinus[140].

Mining activities, including underground extraction, waste dumping, coal transport, and coking-related emissions, have indirect impacts on paramos as they mobilize pollutants, including heavy metals from coal deposits[49]. Detection of contaminants surpassing acceptable limits near mining sites, coupled with mining licenses covering all of Rabanal and parts of Guerrero, underscores the inadequacy of environmental regulations[49,110,141]. Remote sensing provides a tool for detecting compound pollution sources and monitoring environmental degradation due to mining, which could support evidence-based decision-making and targeted interventions to safeguard ecological integrity.

Local inhabitants have raised concerns about the effects of coal mining on water supply, human health, and biodiversity. Underground mining affects groundwater reserves, while improper waste disposal leads to soil and water contamination[142–144]. Inefficient coking technologies generate air pollution[145], with coal ash and dust affecting soil and water quality[146]. Field observations reveal that the vegetation in the study area is covered with black soot from nearby coke ovens and coal dust on adjacent dirt roads, exacerbated by frequent truck traffic on unpaved roads adjacent to the paramo; effects that have also been documented in China's Changhe River mining areas[147]. The affected vegetation showed a decrease in the red and near-infrared reflectance[147,148], which in addition to demonstrating a reduction in the natural albedo, likely signals a deterioration in the paramo ecosystem's health.

Climate change

In addition to the local and regional forces driving continuous native vegetation loss, global factors such as climate change are also pressuring paramo ecosystems[27]. Prior to 2008, the mean maximum temperature in the region increased 0.2–0.4 °C per decade, with projections suggesting a 3.0 ± 1.5 °C rise and decreasing precipitation by the next century, exacerbating water stress[121]. Rising temperatures and changing precipitation patterns induce shifts in paramo boundaries, causing upward migration even without direct human interference[149], as observed in the Ecuadorian Andes[150,151], and Colombia's paramo Chingaza[152]. Although no significant trends in precipitation variability were identified[149,153], increased seasonal wildfires are expected due to the intensification of the El Niño–Southern Oscillation[154–156]. Paramos, being fire-prone ecosystems, experience frequent burning due to human activities, particularly during the hot, dry season between January and March[157]. An unprecedented wildfire season is currently in progress, devastating Colombia's paramos[158].

A comparison of paramo vegetation distribution between 1984 and 2021 reveals significant altitudinal differences. While paramo Rabanal showed a reduced, but still peak, concentration of paramo vegetation between approximately 3350 to 3400 mamsl, there's a decline in coverage between 3180 to 3320 mamsl. Similarly, paramo Guerrero shows a reduction in coverage in the same altitude range, with a peak concentration shift from ~ 3250 m to ~ 3600 m, indicating a 94.6-m per decade upward migration. Consequently, paramo vegetation recedes as montane vegetation expands, facilitated by rising temperatures that favour agricultural activities at progressively higher altitudes[159].

It has been suggested that paramos are increasingly vulnerable to disturbances caused by human activities, which inherently decrease biodiversity. This vulnerability is compounded by the naturally narrow range of eco-physiological strategies available to species in these ecosystems, because of the extremely harsh environmental conditions they face. The presence of multiple species sharing similar traits is essential for maintaining resilience in these ecosystems[160]; yet climate change has also led to the proliferation of invasive species such as Gorse (*Ulex europaeus*)[161,162]. Known for its adaptability and use of fire for dispersal[163], Gorse probably accounts for much of the observed increase in montane vegetation within the paramos[15,164]. Moreover, due to their high nitrogen intake, the species disrupts the natural nitrogen cycle, causing rapid soil degradation and hindering the survival, germination, and growth of other species[165]. Gorse quickly removes water from the ecosystem, altering its hydrological balance and causing further water stress[166]; so in spite of the presence of vegetation, the ecosystem's ecological function is lost. The paramos' high solar radiation along with the presence of fire-prone invasive species increase fire risk by drying out herbaceous vegetation[167], raising the probability of spontaneous combustion of organic material[168,169].

Monitoring paramos

Several regions face pressing issues despite their formal designation as protected areas, and their delineation remains incomplete[170]. Establishing consistent paramo boundaries is crucial for their protection, and monitoring their extent and health will both create awareness of their vulnerability and help identify the highest impact human activities. The existing regulatory framework is failing to protect paramos because of lack of enforcement and systematic monitoring, as we see from the issuance of mining titles within protected paramos.

Efforts towards restoration have had some success in reversing paramo degradation[171], for example, in Chingaza National Natural Park. This shows that recovery may be possible, but biodiversity is still reduced compared to unaltered paramos[128], indicating the most effective conservation strategy is to prevent further damage in existing paramos. Large-scale monitoring from space provides a cost-effective way to assess current ecological status and identify vulnerable areas. Composite techniques must be applied to address persistent cloud coverage and integrating data from multiple satellites[172], enhances coverage, temporal, and spatial resolution, so they can be used as a starting point for local field studies and inform targeted conservation initiatives.

Introducing a new approach to assess vegetation health will enhance the parameters that can be remotely monitored in paramos. This could not only reinforce local conservation efforts but also deepen global environmental understanding. Given the sensitivity of paramo ecosystems to human activities and climate change, this monitoring approach can be adapted for similar high-altitude ecosystems worldwide. The insights gained from our study can be used to develop a comprehensive monitoring program for paramo vegetation health, inform conservation practices, and contribute to broader ecological research and preservation efforts.

Conclusions

Paramos are fragile ecosystems that easily suffer degradation from LULC changes. Fortunately, there is an increasing recognition of the need to protect them, and new policies promote their integrality, preservation, and restoration. However, the upward shift of paramo vegetation's lower limits, leading to an evolving delineation of paramo boundaries, could potentially threaten these vital ecosystems with extinction. If the current trend continues, by 2040, only 30% of paramo Guerrero's native vegetation will remain. By 2085, it is projected that all paramo vegetation cover will be lost, assuming wildfires do not hasten this process. It is thus imperative to incorporate the effects of climate change in decision-making to preserve the ability of paramos to provide ecosystem services.

In recent years, the pace of LULC changes within paramos has decelerated, possibly due to increasingly effective preservation efforts and/or a decrease in pressure exerted by communities. However, the repercussions of changes within and around these ecosystems over the past four decades are already being felt by communities. These include a reduction in paramo extent, fragmentation, conflicts over water use, atmospheric pollution, soil degradation, water contamination, and deteriorating vegetation health. The impact of soot and dust on the health of paramo vegetation and its water retention capacity is a subject that requires further exploration. Monitoring changes in the spectral signature of vegetation can provide valuable insights for field studies and guide protective measures.

Low-cost remote sensing tools provide an efficient means to monitor land changes, track environmental trends, and facilitate informed decision-making. Specifically, monitoring invasive species like Gorse within paramo areas can aid in their location, control, and eradication, thereby enhancing paramo conservation strategies. The need for continued monitoring of LULC changes is paramount, and extending this monitoring to other paramos is crucial. This will help raise awareness and concentrate social, economic, and ecological strategies towards consistently defining and protecting these vulnerable ecosystems. Such measures will prevent further decline and safeguard biodiversity and potable water supply.

Data availability

In addition to the Supplementary Information, the supervised classification and change detection maps produced as part of our analyses are available for download as georeferenced layer files in the following online repository:

Murad, Cesar (2024), "Repository of land use and land cover maps for the paramos Rabanal and Guerrero in Central Colombia", Mendeley Data, V1, https://doi.org/10.17632/gvkm5wf3s5.1.

Received: 3 April 2024; Accepted: 12 July 2024
Published online: 19 July 2024

References

1. Hofstede, R., Segarra, P. & Mena, P. *Los Páramos del Mundo* (Proyecto Atlas Mundial de los Páramos. Global Peatland Initiative/NC-IUCN/EcoCiencia, Quito, 2003).
2. Luteyn, J. L. Páramos: A checklist of plant diversity, geographical distribution, and botanical literature. *Mt. Res. Dev.* **20**, 99–100 (2000).
3. Mosquera, G. M. *et al.* Frontiers in páramo water resources research: A multidisciplinary assessment. *Sci. Total Environ.* **892**, 164373 (2023).
4. Morales, M. *et al. Atlas de Páramos de Colombia* (Instituto de Investigación de Recursos Biológicos Alexander von Humboldt, 2007).
5. Benavides, J. C., Rocha, S. & Blanco, E. A. Spatial and temporal patterns of methane emissions from mountain peatlands in the northern Andes across a disturbance gradient. *Front. Earth Sci.* **11**, (2023).
6. Rivera Ospina, D. & Rodríguez Murcia, C. E. *Guía divulgativa de criterios para la delimitación de páramos de Colombia* (Ministerio de Ambiente, Vivienda y Desarrollo Territorial: Instituto de Investigación de Recursos Biológicos Alexander Von Humboldt, Bogotá, 2011).
7. Cuatrecasas, J. Aspectos de la vegetación natural de Colombia. *Revista de la Academia Colombiana de Ciencias Exactas, Físicas y Naturales* **10**, 221–268 (1958).
8. Cuatrecasas, J. Observaciones geobotánicas en Colombia. *Trab* **27**, 144 (1934).
9. Van der Hammen, T. Páramos. *Informe nacional sobre el estado de la biodiversidad* 10–37 (1997).
10. Guhl, E. *Los Páramos Circundantes de La Sabana de Bogotá* (Jardín Botánico" José Celestino Mutis", 1982).
11. Rangel, J. O. Diversidad biótica III: La región de vida paramuna. *Bogotá: Universidad Nacional de Colombia, Facultad de Ciencias, Instituto de Ciencias Naturales & Instituto de investigación de recursos biológicos Alexander von Humboldt* (2000).
12. Medina, G. & Mena, P. Los páramos en el Ecuador. *Los Páramos del Ecuador. Particularidades, Problemas y Perspectivas. Proyecto Páramo. Quito. Fundación Ecuatoriana de Estudios Ecológicos* (2001).
13. Cortés-Duque, J., Pinzón, S., Enrique, C., Mejía, S. & Patricia, A. *Aportes a la conservación estratégica de los páramos de Colombia: actualizacion de la cartografia de los complejos de páramo a escala 1:100.000* (Instituto de Investigación de Recursos Biológicos Alexander von Humboldt, 2013).
14. Cuatrecasas, J. Páramo vegetation and its life forms. *Colloquium Geographicum* **9**, 163–186 (1968).
15. Cortés-Duque, J., Sarmiento Pinzón, C. E., & IAvH488. *Visión socioecosistémica de los páramos y la alta montaña colombiana. Memorias del proceso de definición de criterios para la delimitación de páramos* (Instituto de Investigación de Recursos Biológicos Alexander von Humboldt, 2013).
16. Ministerio del Medio Ambiente. Programa para el Manejo Sostenible y Restauración de Ecosistemas de la Alta Montaña colombiana. (2002).
17. Buytaert, W. *et al.* Human impact on the hydrology of the Andean páramos. *Earth Sci. Rev.* **79**, 53–72 (2006).
18. Leroy, D. Farmers' perceptions of and adaptations to water scarcity in Colombian and Venezuelan Páramos in the context of climate change. *mred* **39**, R21–R34 (2019).
19. Tapia, C. *Plan participativo de manejo y conservación del macizo del Páramo de Rabanal* (IAVH, 2009).
20. Ruiz, D., Moreno, H. A., Gutiérrez, M. E. & Zapata, P. A. Changing climate and endangered high mountain ecosystems in Colombia. *Sci. Total Environ.* **398**, 122–132 (2008).
21. Chaminé, H. I., Pereira, A. J. S. C., Teodoro, A. C. & Teixeira, J. Remote sensing and GIS applications in earth and environmental systems sciences. *SN Appl. Sci.* **3**, 870 (2021).
22. Willis, K. S. Remote sensing change detection for ecological monitoring in United States protected areas. *Biol. Conserv.* **182**, 233–242 (2015).
23. Jaafari, S., Sakieh, Y., Shabani, A. A., Danehkar, A. & Nazarisamani, A. Landscape change assessment of reservation areas using remote sensing and landscape metrics (case study: Jajroud reservation, Iran). *Environ. Dev. Sustain.* **18**, 1701–1717 (2016).
24. Jiang, F., Zhang, Y., Li, J. & Sun, Z. Research on remote sensing ecological environmental assessment method optimized by regional scale. *Environ. Sci. Pollut. Res.* **28**, 68174–68187 (2021).
25. De Araujo Barbosa, C. C., Atkinson, P. M. & Dearing, J. A. Remote sensing of ecosystem services: A systematic review. *Ecol. Indic.* **52**, 430–443 (2015).
26. Anselm, N., Brokamp, G. & Schütt, B. Assessment of land cover change in Peri-Urban High Andean environments south of Bogotá, Colombia. *Land* **7**, 75 (2018).
27. Clerici, N., Cote-Navarro, F., Escobedo, F. J., Rubiano, K. & Villegas, J. C. Spatio-temporal and cumulative effects of land use-land cover and climate change on two ecosystem services in the Colombian Andes. *Sci. Total Environ.* **685**, 1181–1192 (2019).
28. Peyre, G., Osorio, D., François, R. & Anthelme, F. Mapping the páramo land-cover in the Northern Andes. *Int. J. Remote Sens.* **42**, 7777–7797 (2021).
29. Rodríguez-Aparicio, J. A. & Vergara-Buitrago, P. A. Environmental analysis of coal mining in the strategic ecosystem of paramo (Boyacá, Colombia). *Sci. Tech.* **26**, 398–405 (2021).
30. Peña, Q. A. J. *et al.* Trend analysis to determine hazards related to climate change in the Andean agricultural areas of Cundinamarca and Boyacá. *Agronomía Colombiana* **29**, 467–478 (2011).
31. Agudelo Sedano, R. Áreas Protegidas Con Ecosistemas De Páramo Y Gestión De La RAPE Región Central. Oficina Asesora de Planeación Institucional (2018).
32. Mora Pacheco, K. G. Agriculture and Livestock in Wetlands in the Bogota Plateau (Colombia), Eighteenth Century. Land use and wetland management. In *Environmental History in the Making: Volume II: Acting* (eds. Joanaz de Melo, C., Vaz, E. & Costa Pinto, L. M.) 3–13 (Springer International Publishing, 2017). https://doi.org/10.1007/978-3-319-41139-2_1.
33. Rubio, T., Tapia, C., Urdaneta, M. Estudio sobre el estado actual del macizo del páramo de Rabanal. (2008).
34. Rodríguez, N. L. El páramo de guerrero: conflictos entre conservación y reprimarización de su economía. *Revista Geográfica de América Central* **2**, (2011).
35. Carvajal, J. H. & Navas, O. Bogotá "Savanna". In *Landscapes and Landforms of Colombia* (ed. Hermelin, M.) 115–126 (Springer International Publishing, 2016). https://doi.org/10.1007/978-3-319-11800-0_10.
36. Hofstede, R. *et al. Los Páramos Andinos?¿Qué Sabemos? Estado de Conocimiento Sobre El Impacto Del Cambio Climático En El Ecosistema Páramo* (Quito, Ecuador., 2014).
37. Urrea, V., Ochoa, A. & Mesa, O. Seasonality of rainfall in Colombia. *Water Resour. Res.* **55**, 4149–4162 (2019).
38. Castañeda-Martín, A. E. & Montes-Pulido, C. R. Carbon stock in andean paramo. *Entramado* **13**, 210–221 (2017).

39. Gastauer, M., Thiele, J., Porembski, S. & Neri, A. V. How do altitude and soil properties influence the taxonomic and phylogenetic structure and diversity of Brazilian páramo vegetation?. *J. Mt. Sci.* **17**, 1045–1057 (2020).
40. Díaz-Granados Ortiz, M. A., Navarrete González, J. D. & Suárez López, T. Páramos: Hidrosistemas sensibles. *Revista de Ingeniería* 64–75 (2005).
41. Madriñán, S., Cortés, A. J. & Richardson, J. E. Páramo is the world's fastest evolving and coolest biodiversity hotspot. *Front. Genet.* **4**, (2013).
42. Peyre, G., Balslev, H. & Font, X. Phytoregionalisation of the Andean páramo. *PeerJ* **6**, e4786 (2018).
43. Peyre, G. Plant diversity and vegetation of the Andean Páramo. *Tesis Doctorals—Facultat—Biologia* (2015).
44. Lis-Gutiérrez, M., Rubiano-Sanabria, Y. & Loaiza-Usuga, J. C. Soils and land use in the study of soil organic carbon in Colombian highlands catena. *AUC Geographica* **54**, 15–23 (2019).
45. Sarmiento Perez, G. A. S. & Guatame, C. L. Interpretación del Ambiente Sedimentario de los Carbones de la Formación Guaduas en el Sinclinal Checua-Lenguazaque apartir del análisis petrográfico. *Geol. Colomb.* **29**, 41–58 (2004).
46. Mariño, M. J. & Amaya, E. Lithofacies cyclicity determination in the guaduas formation (Colombia) using Markov chains. *Earth Sci. Res. J.* **20**, B1–B9 (2016).
47. Mariño-Martínez, J. E. *et al.* Emisiones de metano asociadas a la minería subterránea del carbón en el altiplano cundiboyacense (Colombia). *Revista de la Academia Colombiana de Ciencias Exactas, Físicas y Naturales* **45**, 864–874 (2021).
48. Moore, T. A. *et al.* Petrographic and geochemical characteristics of selected coal seams from the Late Cretaceous-Paleocene Guaduas Formation, Eastern Cordillera Basin, Colombia. *Int. J. Coal Geol.* **259**, 104042 (2022).
49. González-Martínez, M. D., Huguet, C., Pearse, J., McIntyre, N. & Camacho, L. A. Assessment of potential contamination of Paramo soil and downstream water supplies in a coal-mining region of Colombia. *Appl. Geochem.* **108**, 104382 (2019).
50. Mohanty, A., Chakladar, S., Mallick, S. & Chakravarty, S. Structural characterization of coking component of an Indian coking coal. *Fuel* **249**, 411–417 (2019).
51. Robineau, O., Châtelet, M., Soulard, C.-T., Michel-Dounias, I. & Posner, J. Integrating farming and Páramo conservation: A case study From Colombia. *mred* **30**, 212–221 (2010).
52. Vermote, E., Justice, C., Claverie, M. & Franch, B. Preliminary analysis of the performance of the Landsat 8/OLI land surface reflectance product. *Remote Sens. Environ.* **185**, 46–56 (2016).
53. Kuhn, C. *et al.* Performance of Landsat-8 and Sentinel-2 surface reflectance products for river remote sensing retrievals of chlorophyll-*a* and turbidity. *Remote Sens. Environ.* **224**, 104–118 (2019).
54. Claverie, M., Vermote, E. F., Franch, B. & Masek, J. G. Evaluation of the Landsat-5 TM and Landsat-7 ETM + surface reflectance products. *Remote Sens. Environ.* **169**, 390–403 (2015).
55. Campos-Taberner, M. *et al.* Understanding deep learning in land use classification based on Sentinel-2 time series. *Sci. Rep.* **10**, 17188 (2020).
56. Louis, J. *et al.* Sentinel-2 global surface reflectance level-2A product generated with Sen2Cor. In *IGARSS 2019–2019 IEEE International Geoscience and Remote Sensing Symposium* 8522–8525 (IEEE, 2019). https://doi.org/10.1109/IGARSS.2019.8898540.
57. Main-Knorn, M. *et al.* Sen2Cor for Sentinel-2. In *Image and Signal Processing for Remote Sensing XXIII* vol. 10427 37–48 (SPIE, 2017).
58. Knudby, A. *et al.* Using multiple Landsat scenes in an ensemble classifier reduces classification error in a stable nearshore environment. *Int. J. Appl. Earth Observ. Geoinf.* **28**, 90–101 (2014).
59. Claverie, M. *et al.* The Harmonized Landsat and Sentinel-2 surface reflectance data set. *Remote Sens. Environ.* **219**, 145–161 (2018).
60. Anaya, J. A. *et al.* Drivers of forest loss in a megadiverse hotspot on the Pacific coast of Colombia. *Remote Sens.* **12**, 1235 (2020).
61. Anderson, J. R. *A Land Use and Land Cover Classification System for Use with Remote Sensor Data* (Government Printing Office, 1976).
62. Rodríguez Eraso, N., Armenteras-Pascual, D. & Alumbreros, J. R. Land use and land cover change in the Colombian Andes: Dynamics and future scenarios. *J. Land Use Sci.* **8**, 154–174 (2013).
63. Balthazar, V., Vanacker, V., Molina, A. & Lambin, E. F. Impacts of forest cover change on ecosystem services in high Andean mountains. *Ecol. Indic.* **48**, 63–75 (2015).
64. Ross, C., Fildes, S. & Millington, A. Land-use and land-cover change in the Páramo of South-Central Ecuador, 1979–2014. *Land* **6**, 46 (2017).
65. Acevedo, C. J. D., Romero-Alarcon, L. V. & Miranda-Esquivel, D. R. Páramos Neotropicales como unidades biogeográficas. *Revista de Biología Tropical* **68**, 503–516 (2020).
66. Jiménez-Rivillas, C., García, J. J., Quijano-Abril, M. A., Daza, J. M. & Morrone, J. J. A new biogeographical regionalisation of the Páramo biogeographic province. *Aust. Syst. Bot.* **31**, 296–310 (2018).
67. Duadze, S. E. K. *Land Use and Land Cover Study of the Savannah Ecosystem in the Upper West Region (Ghana) Using Remote Sensing*, vol. 16 (Cuvillier Verlag, 2004).
68. Mountrakis, G., Im, J. & Ogole, C. Support vector machines in remote sensing: A review. *ISPRS J. Photogramm. Remote Sens.* **66**, 247–259 (2011).
69. Nong, D. H., Fox, J., Miura, T. & Saksena, S. Built-up area change analysis in Hanoi using support vector machine classification of landsat multi-temporal image stacks and population data. *Land* **4**, 1213–1231 (2015).
70. Li, C., Wang, J., Wang, L., Hu, L. & Gong, P. Comparison of classification algorithms and training sample sizes in urban land classification with landsat thematic mapper imagery. *Remote Sens.* **6**, 964–983 (2014).
71. Gómez, C., White, J. C. & Wulder, M. A. Optical remotely sensed time series data for land cover classification: A review. *ISPRS J. Photogramm. Remote Sens.* **116**, 55–72 (2016).
72. Phiri, D. *et al.* Sentinel-2 data for land cover/use mapping: A review. *Remote Sens.* **12**, 2291 (2020).
73. Lang, S. Object-based image analysis for remote sensing applications: modeling reality—Dealing with complexity. In *Object-Based Image Analysis: Spatial Concepts for Knowledge-Driven Remote Sensing Applications* (eds. Blaschke, T., Lang, S. & Hay, G. J.) 3–27 (Springer, 2008). https://doi.org/10.1007/978-3-540-77058-9_1.
74. Dingle Robertson, L. & King, D. J. Comparison of pixel- and object-based classification in land cover change mapping. *Int. J. Remote Sens.* **32**, 1505–1529 (2011).
75. Marangoz, A. M., Sekertekin, A. & Akçin, H. Analysis of land use land cover classification results derived from sentinel-2 image. In *Proceedings of the 17th International Multidisciplinary Scientific GeoConference Surveying Geology and Mining Ecology Management, SGEM* 25–32 (2017).
76. Butt, A., Shabbir, R., Ahmad, S. S. & Aziz, N. Land use change mapping and analysis using Remote Sensing and GIS: A case study of Simly watershed, Islamabad, Pakistan. *Egypt. J. Remote Sens. Space Sci.* **18**, 251–259 (2015).
77. Kandrika, S. & Roy, P. S. Land use land cover classification of Orissa using multi-temporal IRS-P6 awifs data: A decision tree approach. *Int. J. Appl. Earth Observ. Geoinf.* **10**, 186–193 (2008).
78. Thorat, S. S., Rajendra, Y. D., Kale, K. V. & Mehrotra, S. C. Estimation of crop and forest areas using expert system based knowledge classifier approach for Aurangabad district. *Int. J. Comput. Appl.* **121**, (2015).
79. Manandhar, R., Odeh, I. O. A. & Ancev, T. Improving the accuracy of land use and land cover classification of landsat data using post-classification enhancement. *Remote Sens.* **1**, 330–344 (2009).

80. Rwanga, S. S. & Ndambuki, J. M. Accuracy assessment of land use/land cover classification using remote sensing and GIS. *Int. J. Geosci.* **8**, 611–622 (2017).
81. Yuan, F., Sawaya, K. E., Loeffelholz, B. C. & Bauer, M. E. Land cover classification and change analysis of the Twin Cities (Minnesota) Metropolitan Area by multitemporal Landsat remote sensing. *Remote Sens. Environ.* **98**, 317–328 (2005).
82. Tilahun, A. & Teferie, B. Accuracy assessment of land use land cover classification using Google Earth. *Am. J. Environ. Prot.* **4**, 193–198 (2015).
83. Eskandari, S., Reza Jaafari, M., Oliva, P., Ghorbanzadeh, O. & Blaschke, T. Mapping land cover and tree canopy cover in Zagros Forests of Iran: Application of Sentinel-2, google earth, and field data. *Remote Sens.* **12**, 1912 (2020).
84. Coppin, P., Lambin, E., Jonckheere, I. & Muys, B. Digital change detection methods in natural ecosystem monitoring: A review. In *Analysis of Multi-Temporal Remote Sensing Images* vol. 2 3–36 (World Scientific, 2002).
85. Hecheltjen, A., Thonfeld, F. & Menz, G. Recent advances in remote sensing change detection—A review. In *Land Use and Land Cover Mapping in Europe: Practices & Trends* (eds. Manakos, I. & Braun, M.) 145–178 (Springer Netherlands, 2014). https://doi.org/10.1007/978-94-007-7969-3_10.
86. Dewan, A. M. & Yamaguchi, Y. Land use and land cover change in Greater Dhaka, Bangladesh: Using remote sensing to promote sustainable urbanization. *Appl. Geogr.* **29**, 390–401 (2009).
87. Rawat, J. S. & Kumar, M. Monitoring land use/cover change using remote sensing and GIS techniques: A case study of Hawalbagh block, district Almora, Uttarakhand, India. *Egypt. J. Remote Sens. Space Sci.* **18**, 77–84 (2015).
88. Cracknell, A. P. & Mansor, S. B. Detection of sub-surface coal fires using Landsat Thematic Mapper data. *Int. Arch. Photogramm. Remote Sens.* **29**, 750–750 (1993).
89. Zhao, L. *et al.* Investigating the impact of using IR bands on early fire smoke detection from landsat imagery with a lightweight CNN model. *Remote Sens.* **14**, 3047 (2022).
90. Afira, N. & Wijayanto, A. W. Mono-temporal and multi-temporal approaches for burnt area detection using Sentinel-2 satellite imagery (a case study of Rokan Hilir Regency, Indonesia). *Ecol. Inform.* **69**, 101677 (2022).
91. Ayele, G. T. *et al.* Time series land cover mapping and change detection analysis using geographic information system and remote sensing, Northern Ethiopia. *Air Soil Water Res.* (2018) https://doi.org/10.1177/1178622117751603.
92. Sonnenschein, R., Kuemmerle, T., Udelhoven, T., Stellmes, M. & Hostert, P. Differences in Landsat-based trend analyses in drylands due to the choice of vegetation estimate. *Remote Sens. Environ.* **115**, 1408–1420 (2011).
93. Vittek, M., Brink, A., Donnay, F., Simonetti, D. & Desclée, B. Land cover change monitoring using landsat MSS/TM satellite image data over West Africa between 1975 and 1990. *Remote Sens.* **6**, 658–676 (2014).
94. Cox, D. R. & Stuart, A. Some quick sign tests for trend in location and dispersion. *Biometrika* **42**, 80–95 (1955).
95. Colditz, R. R. *et al.* Potential effects in multi-resolution post-classification change detection. *Int. J. Remote Sens.* **33**, 6426–6445 (2012).
96. Curatola Fernández, G. F. *et al.* Land cover change in the Andes of Southern Ecuador—Patterns and drivers. *Remote Sens.* **7**, 2509–2542 (2015).
97. Loaiza-Usuga, J. C., Lis-Gutiérrez, M. & Rubiano-Sanabria, Y. Chapter 7—Land use and environmental changes in the Andean Paramo soils. In *Climate and Land Use Impacts on Natural and Artificial Systems* (ed. Nistor, M.-M.) 105–134 (Elsevier, 2021). https://doi.org/10.1016/B978-0-12-822184-6.00014-4.
98. Blake, L. J., Chohan, J. K. & Escobar, M. P. Agro-extractivism and neoliberal conservation: *campesino* abandonment in the Boyacá páramos, Colombia. *J. Rural Stud.* **102**, 103071 (2023).
99. Murad, C. A. & Pearse, J. Landsat study of deforestation in the Amazon region of Colombia: Departments of Caquetá and Putumayo. *Remote Sens. Appl. Soc. Environ.* **11**, 161–171 (2018).
100. Fernandez, N. & Camacho, L. A. Coupling hydrological and water quality models for assessing coal mining impacts on surface water resources. 5145–5154 (2019). https://doi.org/10.3850/38WC092019-1700.
101. Solanilla, M., Díaz, J. L., Varela, J. D. & Ordoñez, W. Vida digna, justicia ambiental y social: el debate alrededor de los páramos. *Revista Semillas* **5** (2021).
102. Bremer, L. L. *et al.* Biodiversity outcomes of payment for ecosystem services: Lessons from páramo grasslands. *Biodivers. Conserv.* **28**, 885–908 (2019).
103. Duarte-Abadía, B. & Boelens, R. Disputes over territorial boundaries and diverging valuation languages: The Santurban hydrosocial highlands territory in Colombia. *Water Int.* **41**, 15–36 (2016).
104. Sands, A. Regulatory chill and domestic law: Mining in the Santurbán Páramo. *World Trade Rev.* **22**, 55–72 (2023).
105. Aguilar-Pesantes, A., Peña Carpio, E., Vitvar, T., Koepke, R. & Menéndez-Aguado, J. M. A comparative study of mining control in Latin America. *Mining* **1**, 6–18 (2021).
106. González-González, A., Clerici, N. & Quesada, B. Growing mining contribution to Colombian deforestation. *Environ. Res. Lett.* **16**, 064046 (2021).
107. Rodríguez-Zapata, M. A. & Ruiz-Agudelo, C. A. Environmental liabilities in Colombia: A critical review of current status and challenges for a megadiverse country. *Environ. Chall.* **5**, 100377 (2021).
108. Gutiérrez-Gómez, L. Mining in Colombia: Tracing the harm of neoliberal policies and practices. In *Environmental Crime in Latin America: The Theft of Nature and the Poisoning of the Land* (eds. Rodríguez Goyes, D., Mol, H., Brisman, A. & South, N.) 85–113 (Palgrave Macmillan UK, 2017). https://doi.org/10.1057/978-1-137-55705-6_5.
109. Ungar, P. Assembling an ecosystem: The making of state páramos in Colombia. *Conserv. Soc.* **19**, 119–129 (2021).
110. Alonso, D. L., Pérez, R., Okio, C. K. Y. A. & Castillo, E. Assessment of mining activity on arsenic contamination in surface water and sediments in southwestern area of Santurbán paramo, Colombia. *J. Environ. Manag.* **264**, 110478 (2020).
111. Prieto, G. & Duitama, L. M. Acid drainage of coal mining in Cundinamarca Department, Colombia. In *Environmental Geochemistry in Tropical and Subtropical Environments* (eds. Drude de Lacerda, L., Santelli, R. E., Duursma, E. K. & Abrão, J. J.) 125–134 (Springer, 2004). https://doi.org/10.1007/978-3-662-07060-4_11.
112. Patiño, S. *et al.* Influence of land use on hydro-physical soil properties of Andean páramos and its effect on streamflow buffering. *CATENA* **202**, 105227 (2021).
113. Zapata, A. *et al.* Páramo lakes of Colombia: An overview of their geographical distribution and physicochemical characteristics. *Water* **13**, 2175 (2021).
114. Páez, A. M. & Vallejo Piedrahíta, C. Channeling water conflicts through the legislative branch in Colombia. *Water* **13**, 1214 (2021).
115. Murtinho, F., Tague, C., de Bievre, B., Eakin, H. & Lopez-Carr, D. Water scarcity in the andes: A comparison of local perceptions and observed climate, land use and socioeconomic changes. *Hum. Ecol.* **41**, 667–681 (2013).
116. Bogotá-A, R. G., Hooghiemstra, H. & Berrio, J. C. North Andean environmental and climatic change at orbital to submillennial time-scales: Vegetation, water-levels and sedimentary regimes from Lake Fúquene between 284 and 130ka. *Rev. Palaeobot. Palynol.* **226**, 91–107 (2016).
117. de Car, C. C. & Ambiotec, U. Elaboracion De Los Estudios De Diagnostico Prospectiva Y Formulacion Para La Cuenca Hidrigráfica De Los Rios Ubaté Y Suárez (Departamento De Cundinamarca). *Cuenca Alto Rio Ubate 2401* **2**, (2006).
118. Arboleda Valencia, J. W., Castro Ortegón, D. C. & Betancur Pérez, J. F. Reflections on the Process of Declaring the Fuquene Lagoon as a Protected Area and Inclusion to the Protected Areas National System. *J. Hunan Univ. Nat. Sci.* **49**, (2022).

119. Salgado, J. *et al.* Long-term habitat degradation drives neotropical macrophyte species loss while assisting the spread of invasive plant species. *Front. Ecol. Evol.* **7**, (2019).
120. Valencia Perez, M. A., Sorzano López, C. & Biotierra, F. Plan guia de manejo sitios de interes ambiental con potencial ecoturístico del Municipio de Suesca. (2017).
121. Buytaert, W., Cuesta-Camacho, F. & Tobón, C. Potential impacts of climate change on the environmental services of humid tropical alpine regions. *Glob. Ecol. Biogeogr.* **20**, 19–33 (2011).
122. Partap, T. Hill agriculture: Challenges and opportunities. *Indian J. Agric. Econ.* **66**, (2011).
123. Vandermeer, J. *et al.* Effects of industrial agriculture on global warming and the potential of small-scale agroecological techniques to reverse those effects. *New World Agric. Ecol. Group.* (2009).
124. Uribe, N., Corzo, G., Quintero, M., van Griensven, A. & Solomatine, D. Impact of conservation tillage on nitrogen and phosphorus runoff losses in a potato crop system in Fuquene watershed, Colombia. *Agric. Water Manag.* **209**, 62–72 (2018).
125. Vargas, G., León, N. & Hernández, Y. Agricultural socio-economic effects in colombia due to degradation of soils. In *Sustainable Management of Soil and Environment* (eds. Meena, R. S., Kumar, S., Bohra, J. S. & Jat, M. L.) 289–337 (Springer, 2019). https://doi.org/10.1007/978-981-13-8832-3_9.
126. Etter, A., McAlpine, C. & Possingham, H. Historical patterns and drivers of landscape change in Colombia since 1500: A regionalized spatial approach. *Ann. Assoc. Am. Geogr.* **98**, 2–23 (2008).
127. Sanchez-Cuervo, A. M. & Aide, T. M. Identifying hotspots of deforestation and reforestation in Colombia (2001–2010): Implications for protected areas. *Ecosphere* **4**, art143 (2013).
128. Rojas-Zamora, O., Insuasty-Torres, J., de los Cardenas, C. Á. & Vargas Ríos, O. Relocation of Espeletia grandiflora (Asteraceae) plants as a strategy for enrichment of disturbed paramo areas (PNN Chingaza, Colombia). *Rev. Biol. Trop.* **61**, 363–376 (2013).
129. Sarmiento, L., Smith, J. K., Márquez, N., Escalona, A. & Erazo, M. C. Constraints for the restoration of tropical alpine vegetation on degraded slopes of the Venezuelan Andes. *Plant Ecol. Divers.* **8**, 277–291 (2015).
130. Avellaneda-Torres, L. M., León Sicard, T. E. & Torres Rojas, E. Impact of potato cultivation and cattle farming on physicochemical parameters and enzymatic activities of Neotropical high Andean *Páramo* ecosystem soils. *Sci. Total Environ.* **631–632**, 1600–1610 (2018).
131. Farley, K. A. Grasslands to tree plantations: Forest transition in the Andes of Ecuador. *Ann. Assoc. Am. Geograph.* **97**, 755–771 (2007).
132. Medina-Torres, B., Jonard, M., Rendón, M. & Jacquemart, A.-L. Effects of pine plantation on native Ecuadorian Páramo vegetation. *Forests* **13**, 1499 (2022).
133. Buytaert, W., Iñiguez, V. & Bièvre, B. D. The effects of afforestation and cultivation on water yield in the Andean páramo. *For. Ecol. Manag.* **251**, 22–30 (2007).
134. Farley, K. A., Kelly, E. F. & Hofstede, R. G. M. Soil organic carbon and water retention after conversion of grasslands to pine plantations in the Ecuadorian Andes. *Ecosystems* **7**, 729–739 (2004).
135. Farley, K. A. & Kelly, E. F. Effects of afforestation of a páramo grassland on soil nutrient status. *For. Ecol. Manag.* **195**, 281–290 (2004).
136. Quiroz Dahik, C. *et al.* Contrasting stakeholders' perceptions of pine plantations in the Páramo ecosystem of Ecuador. *Sustainability* **10**, 1707 (2018).
137. Montenegro-Díaz, P., Alvear, R. C., Wilcox, B. P. & Carrillo-Rojas, G. Effects of heavy grazing on the microclimate of a humid grassland mountain ecosystem: Insights from a biomass removal experiment. *Sci. Total Environ.* **832**, 155010 (2022).
138. Salazar, A., Baldi, G., Hirota, M., Syktus, J. & McAlpine, C. Land use and land cover change impacts on the regional climate of non-Amazonian South America: A review. *Glob. Planet. Change* **128**, 103–119 (2015).
139. van Dijk, A. I. J. M. & Keenan, R. J. Planted forests and water in perspective. *For. Ecol. Manag.* **251**, 1–9 (2007).
140. Cano, D., Cacciuttolo, C., Custodio, M. & Nosetto, M. Effects of grassland afforestation on water yield in basins of Uruguay: A spatio-temporal analysis of historical trends using remote sensing and field measurements. *Land* **12**, 185 (2023).
141. Agudelo, C. A., Quiroz-Arcentales, L., García-Ubaqie, J. C., Martínez, R. R. & García-Ubaque, C. A. Evaluación de condiciones ambientales: aire, agua y suelos en áreas de actividad minera en Boyacá, Colombia. *Revista de Salud Pública* **18**, 50–60 (2016).
142. Price, P. & Wright, I. A. Water quality impact from the discharge of coal mine wastes to receiving streams: Comparison of impacts from an active mine with a closed mine. *Water Air Soil Pollut.* **227**, 155 (2016).
143. Wang, S. *et al.* Distribution characteristics, risk assessment, and relevance with surrounding soil of heavy metals in coking solid wastes from coking plants in Shanxi, China. *Environ. Monit. Assess.* **195**, 1399 (2023).
144. Wright, I. A., McCarthy, B., Belmer, N. & Price, P. Subsidence from an underground coal mine and mine wastewater discharge causing water pollution and degradation of aquatic ecosystems. *Water Air Soil Pollut.* **226**, 348 (2015).
145. Lambert, T. W. & Lane, S. Lead, arsenic, and polycyclic aromatic hydrocarbons in soil and house dust in the communities surrounding the Sydney, Nova Scotia, tar ponds. *Environ. Health Perspect.* **112**, 35–41 (2004).
146. Huguet, C. & Widory, D. Evaluation of lead contamination derived from coal mining in Lenguazaque, Colombia (2022).
147. Ma, B., Pu, R., Wu, L. & Zhang, S. Vegetation index differencing for estimating foliar dust in an ultra-low-grade magnetite mining area using landsat imagery. *IEEE Access* **5**, 8825–8834 (2017).
148. Yan, X., Shi, W., Zhao, W. & Luo, N. Estimation of atmospheric dust deposition on plant leaves based on spectral features. *Spectrosc. Lett.* **47**, 536–542 (2014).
149. Cresso, M., Clerici, N., Sanchez, A. & Jaramillo, F. Future climate change renders unsuitable conditions for paramo ecosystems in Colombia. *Sustainability* **12**, 8373 (2020).
150. Peyre, G. *et al.* The fate of páramo plant assemblages in the sky islands of the northern Andes. *J. Veg. Sci.* **31**, 967–980 (2020).
151. Sklenář, P. *et al.* Distribution changes in páramo plants from the equatorial high Andes in response to increasing temperature and humidity variation since 1880. *Alp Bot.* **131**, 201–212 (2021).
152. Sanchez, A., Rey-Sánchez, A. C., Posada, J. M. & Smith, W. K. Interplay of seasonal sunlight, air and leaf temperature in two alpine páramo species, Colombian Andes. *Agric. For. Meteorol.* **253–254**, 38–47 (2018).
153. Rojas, E., Arce, B., Peña, A., Boshell, F. & Ayarza, M. Quantization and interpolation of local trends in temperature and precipitation in the high Andean areas of Cundinamarca and Boyaca (Colombia). *Revista Corpoica-Ciencia y Tecnologia Agropecuarias* **11**, 173–182 (2010).
154. Cai, W. *et al.* Changing El Niño-Southern Oscillation in a warming climate. *Nat. Rev. Earth Environ.* **2**, 628–644 (2021).
155. Ojeda-Flechas, C. D. *et al.* Characterization of comprehensive drought events associated with the ENSO warm phase through satellite images in the Valle del Cauca, Colombia. *DYNA* **87**, 204–214 (2020).
156. Pacheco, J., Solera, A., Avilés, A. & Tonón, M. D. Influence of ENSO on droughts and vegetation in a high mountain equatorial climate basin. *Atmosphere* **13**, 2123 (2022).
157. Borrelli, P., Armenteras, D., Panagos, P., Modugno, S. & Schütt, B. The implications of fire management in the andean paramo: A preliminary assessment using satellite remote sensing. *Remote Sens.* **7**, 11061–11082 (2015).
158. Septer, Q. Unprecedented fire season has raged through one of earth's biodiversity hotspots. *Scientific American* https://www.scientificamerican.com/article/unprecedented-fire-season-has-raged-through-one-of-earths-biodiversity-hotspots/ (2024).
159. Castro-Llanos, F., Hyman, G., Rubiano, J., Ramirez-Villegas, J. & Achicanoy, H. Climate change favors rice production at higher elevations in Colombia. *Mitig. Adapt. Strateg. Glob. Change* **24**, 1401–1430 (2019).
160. Cruz, M. & Lasso, E. Insights into the functional ecology of páramo plants in Colombia. *Biotropica* **53**, 1415–1431 (2021).

161. Christina, M., Limbada, F. & Atlan, A. Climatic niche shift of an invasive shrub (Ulex europaeus): A global scale comparison in native and introduced regions. *J. Plant Ecol.* **13**, 42–50 (2020).
162. Hernández-Lambraño, R. E., González-Moreno, P. & Sánchez-Agudo, J. Á. Towards the top: Niche expansion of Taraxacum officinale and Ulex europaeus in mountain regions of South America. *Austral Ecol.* **42**, 577–589 (2017).
163. Udo, N., Tarayre, M. & Atlan, A. Evolution of germination strategy in the invasive species *Ulex europaeus*. *J. Plant Ecol.* **10**, 375–385 (2017).
164. González-M, R. & López-Camacho, R. Catálogo De Las Plantas Vasculares De Ráquira (Boyacá), Flora Andina En Un Enclave Seco De Colombia. *Colomb. For.* **15**, 55–103 (2012).
165. García, R. A., Fuentes-Ramírez, A. & Pauchard, A. Effects of two nitrogen-fixing invasive plants species on soil chemical properties in south-central Chile. *Gayana. Bot.* **69**, 189–192 (2012).
166. Osorio-Castiblanco, D. F., Peyre, G. & Saldarriaga, J. F. Physicochemical analysis and essential oils extraction of the Gorse (*Ulex europaeus*) and French Broom (*Genista monspessulana*), two highly invasive species in the Colombian Andes. *Sustainability* **12**, 57 (2020).
167. Armenteras Pascual, D. *et al.* Characterising fire spatial pattern interactions with climate and vegetation in Colombia. *Agric. For. Meteorol.* **151**, 279–289 (2011).
168. Piechnik, K., Hofmann, A. & Klippel, A. Self-ignition of forest soil samples demonstrated through hot storage tests. *Fire Mater.* https://doi.org/10.1002/fam.3198 (2024).
169. Restuccia, F., Huang, X. & Rein, G. Self-ignition of natural fuels: Can wildfires of carbon-rich soil start by self-heating?. *Fire Saf. J.* **91**, 828–834 (2017).
170. Serrano Frattali, J. P. The legal status of Colombia's Paramos: the socio-environmental conflicts. *Int. J. Environ. Stud.* **80**, 1299–1310 (2023).
171. Molina Benavides, R. A., Campos Gaona, R., Sánchez Guerrero, H., Giraldo Patiño, L. & Atzori, A. S. Sustainable feedbacks of Colombian Paramos involving livestock, agricultural activities, and sustainable development goals of the Agenda 2030. *Systems* **7**, 52 (2019).
172. Chaves, E. D. M., Picoli, C. A. M. & Sanches, D. I. Recent applications of landsat 8/OLI and Sentinel-2/MSI for land use and land cover mapping: A systematic review. *Remote Sens.* **12**, 3062 (2020).

Author contributions

C.M.: Conceptualization, investigation, figure preparation, and manuscript writing. J.P.: Conceptualization, manuscript writing and revision, supervision, C.H.: Manuscript revision, supervision. All authors reviewed the manuscript.

Competing interests

The authors declare no competing interests.

Additional information

Supplementary Information The online version contains supplementary material available at https://doi.org/10.1038/s41598-024-67563-z.

Correspondence and requests for materials should be addressed to C.A.M. or J.P.

Reprints and permissions information is available at www.nature.com/reprints.

Publisher's note Springer Nature remains neutral with regard to jurisdictional claims in published maps and institutional affiliations.